J Stat Phys (2007) 129: 205–239
DOI 10.1007/s10955-007-9399-5

Dynamo Effect in the Kraichnan Magnetohydrodynamic Turbulence

Heikki Arponen · Peter Horvai

Received: 26 October 2006 / Accepted: 9 August 2007 / Published online: 28 September 2007

Abstract The existence of a dynamo effect in a simplified magnetohydrodynamic model of turbulence is considered when the magnetic Prandtl number approaches zero or infinity. The magnetic field is interacting with an incompressible Kraichnan-Kazantsev model velocity field which incorporates also a viscous cutoff scale. An approximate system of equations in the different scaling ranges can be formulated and solved, so that the solution tends to the exact one when the viscous and magnetic-diffusive cutoffs approach zero. In this approximation we are able to determine analytically the conditions for the existence of a dynamo effect and give an estimate of the dynamo growth rate. Among other things we show that in the large magnetic Prandtl number case the dynamo effect is always present. Our analytical estimates are in good agreement with previous numerical studies of the Kraichnan-Kazantsev dynamo by Vincenzi (J. Stat. Phys. 106:1073–1091, 2002).

Keywords Dynamo · Magnetohydrodynamic · Turbulence · Kraichnan-Kazantsev

1 Introduction

The study of the dynamo effect in short time correlated velocity fields was initiated by Kazantsev in [15], where he derived a Schrödinger equation for the pair correlation function of the magnetic field. However, that equation was still quite difficult to analyze except in some special cases. The large magnetic Prandtl number Batchelor regime was studied by Chertkov et al. [5], with methods of Lagrangian path analysis of [4, 21]. However this approach is valid only for limited time (until the finiteness of the velocity field's viscous scale becomes relevant) even for infinitesimal magnetic fields. For the problem involving the full inertial range of the advecting velocity field, Vergassola [22] has obtained the zero

H. Arponen (✉)
Department of Mathematics and Statistics, Helsinki University, P.O. Box 68, 00014 Helsinki, Finland
e-mail: heikki.arponen@helsinki.fi

P. Horvai
Science & Finance, Capital Fund Management, 6-8 Bd Haussmann, 75009 Paris, France

mode exponents in the inertial range (and hence a criterion for presence of the dynamo). Vincenzi [23] obtained numerically (in three dimensional space) the dynamo growth rate at finite magnetic Reynolds and Prandtl numbers. However, until now, an analytical method to obtain the dynamo growth rate was lacking.

Our objective in this paper is to exhibit such a method, derived from the work in [11]. This allows us to better understand the dynamo effect. Last but not least we obtain good approximations to the numerical computation results of Vincenzi.

1.1 From Full MHD to the Kraichnan-Kazantsev Model

Magnetohydrodynamics (MHD) is usually described by the Navier-Stokes equations for a conducting fluid coupled to the magnetic field in the following way:

$$\partial_t \boldsymbol{v} + (\boldsymbol{v}\cdot\nabla)\boldsymbol{v} - \frac{1}{\mu_f\rho_f}(\boldsymbol{B}\cdot\nabla)\boldsymbol{B} + \frac{1}{2\mu_f\rho_f}\nabla(|\boldsymbol{B}|^2) + \frac{1}{\rho_f}\nabla p = \nu_f\Delta\boldsymbol{v} + \boldsymbol{F}, \quad (1.1)$$

$$\partial_t \boldsymbol{B} + (\boldsymbol{v}\cdot\nabla)\boldsymbol{B} - (\boldsymbol{B}\cdot\nabla)\boldsymbol{v} = \frac{1}{\mu_f\sigma_f}\Delta\boldsymbol{B}, \quad (1.2)$$

$$\nabla\cdot\boldsymbol{v} = 0, \quad (1.3)$$

$$\nabla\cdot\boldsymbol{B}, = 0, \quad (1.4)$$

where $\boldsymbol{v}$ and $\boldsymbol{B}$ are the fluid velocity and magnetic (induction) fields respectively, ρ_f is the density of the fluid, μ_f is its magnetic permeability, σ_f its conductivity and ν_f its viscosity, p is the pressure and $\boldsymbol{F}$ may be some externally imposed volume force acting on the fluid. These equations already take into account the so called MHD approximation, whereby the fluid is supposed to be locally charge neutral everywhere, the displacement current is supposed negligible.

In the current paper we will be interested by the growth of an initial seed magnetic field, so we can suppose $\boldsymbol{B}$ to be infinitesimal above. Hence the terms involving $\boldsymbol{B}$ in (1.1) may be neglected (all the more so that they are quadratic). This turns the problem into a passive advection one for the magnetic field (i.e. the magnetic field doesn't influence the evolution of the velocity field), while the velocity field evolves according to the Navier-Stokes equations with some external forcing (independent of the magnetic field).

Since in the passive advection case the velocity field evolves autonomously, one can define for it as usual the Reynolds number $Re = L_v V/\nu_f$, where L_v is the integral scale (scale of largest wavelength excited mode) of the velocity field and V is the typical velocity magnitude at these scales. One can also define a magnetic Reynolds number as $Re_M = VL_v/\kappa$, where $\kappa = 1/(\mu_f\sigma_f)$ is the magnetic diffusivity. Note that L_v is the integral scale of the *velocity* field and V is the *velocity* at such a scale. We will be mostly working in the case where both Reynolds numbers are very large, more specifically in the case when L_v is sent to infinity.

To give an intuitive idea of the dynamo effect, note that, for low values of the magnetic diffusivity (low in the sense that the magnetic Reynolds number based on it is high), the magnetic field lines are approximately frozen into the fluid and they are typically stretched by the flow, due to the term $\boldsymbol{B}\cdot\nabla\boldsymbol{v}$ appearing in (1.2). This process may lead to an exponential growth in time of the magnetic field. If there is such a growth then we talk about turbulent dynamo. If the seed magnetic field is unable to grow, and instead it decays, then we say that there is no dynamo. We point out that this definition is based merely on a linear stability analysis, and does not exclude the possibility of persistent magnetic fields starting from a finite size perturbation, even if the system doesn't show dynamo effect for infinitesimal magnetic fields (reminiscent of the case of hydrodynamic turbulence in a pipe flow).

In addition, we wish to study the situation where the velocity field is turbulent, or in other terms the Reynolds number *Re* is high. Then, using real solutions of the Navier-Stokes equations is only possible for numerical computations.

To deal analyitically with the passive advection problem, a typical way is to resort to some statistical model of the velocity field. We choose here to use the Kraichnan-Kazantsev model [15, 16], because it readily yields to analytical treatment of passive advection [9] and is well understood (see e.g. [3, 8] for a general review, or [1, 12, 22, 23] dealing specifically with the passive turbulent dynamo).

Our problem is now reduced to studying the evolution of $\boldsymbol{B}$ described by

$$\partial_t \boldsymbol{B} + \boldsymbol{v}\cdot\nabla\boldsymbol{B} - \boldsymbol{B}\cdot\nabla\boldsymbol{v} = \kappa\Delta\boldsymbol{B}, \tag{1.5}$$

$$\nabla\cdot\boldsymbol{B} = 0, \tag{1.6}$$

where $\boldsymbol{v}$ is given according to the Kraichnan-Kasantsev model presented below. We will derive an equation for the pair correlation function

$$\left\langle B_i(t,\boldsymbol{r})B_j(t,\boldsymbol{r}')\right\rangle \tag{1.7}$$

averaged over the velocity statistics, and attempt to solve it using a certain approximation scheme, which will be explained at the end of this introduction.

The possible unbounded growth—as we shall see—of the magnetic field's pair correlation function, depending on the roughness parameter ξ (to be defined below) of the velocity field and the magnetic Prandtl number, is in contrast with the passive scalar case, where in the absence of external forcing the dynamics was always dissipative [10, 14, 18].

1.2 Definition of Kraichnan Model

The Kraichnan model is defined as a Gaussian, mean zero, random velocity field, with pair correlation function

$$\begin{aligned}\left\langle v_i(t,\boldsymbol{r})v_j(t',\boldsymbol{r}')\right\rangle &= \delta(t-t')D_0\int \mathrm{d}\!\!^{-}\boldsymbol{k}\,\frac{e^{i\boldsymbol{k}\cdot(\boldsymbol{r}-\boldsymbol{r}')}}{|\boldsymbol{k}|^{d+\xi}}f(l_v|\boldsymbol{k}|)P_{ij}(\boldsymbol{k})\\ &=: \delta(t-t')D_{ij}(\boldsymbol{r}-\boldsymbol{r}';l_v),\end{aligned} \tag{1.8}$$

with $\mathrm{d}\!\!^{-}\boldsymbol{k} := \frac{d^dk}{(2\pi)^d}$ and

$$P_{ij}(\boldsymbol{k}) = \delta_{ij} - \frac{k_ik_j}{k^2} \tag{1.9}$$

to guarantee incompressibility. It is evident that D_{ij} is homogenous and isotropic. We briefly discuss below the meanings of ξ, l_v and f.

The parameter ξ, such that $0 \le \xi \le 2$, describes the roughness of the velocity field. The choice of $\xi = 4/3$ would correspond to the Kolmogorov scaling of equal-time velocity structure functions. However there is no evident prescription for ξ that would best reproduce a real turbulent velocity field, and even for the case under study of passive advection of a magnetic field, it is not clear what ξ should be considered.

The function f is an ultraviolet cutoff, which simulates the effects of viscosity. It decays faster than exponentially at large k, while $f(0) = 1$ and $f'(0) = 0$. For example we could choose $f(l_vk) = \exp(-l_v^2k^2)$, although the explicit form of the function is not needed below.

In the usual case without the cutoff function f the velocity correlation function behaves as a constant plus a term $\propto r^{\xi}$, but in this case we have an additional scaling range for $r \ll l_\nu$ where it scales as $\propto r^2$. The length scale l_ν can be used to define a viscosity ν or alternatively one can use κ to define a length scale l_κ. We can then define the Prandtl number[1] measuring the relative effects of viscosity and diffusivity as $P = \nu/\kappa$. Note that the integral scale was assumed to be infinite, i.e. there is no IR cutoff.

1.3 Plan of the Paper

The goal of the present paper is to extend previous considerations by introducing a set of approximate equations, which admit an exact analytical solution. The analysis proceeds along the same lines as in a previous paper for a different problem by one of us [11]. The problem in the analysis can be traced to existence of length scales dividing the equation in different scaling ranges. In our case there are two such length scales, one arising from the diffusivity κ and the other from the UV cutoff in the velocity correlation function. As will be seen in Appendix 1, what one actually needs in the analysis is the velocity *structure* function defined as

$$\begin{aligned}
&\frac{1}{2}\big\langle (v_i(t,\boldsymbol{r}) - v_i(t,\boldsymbol{r}'))(v_j(t',\boldsymbol{r}) - v_j(t',\boldsymbol{r}'))\big\rangle \\
&\quad = \delta(t-t')D_0 \int \mathrm{d}\boldsymbol{k}\, \frac{1 - e^{i\boldsymbol{k}\cdot(\boldsymbol{r}-\boldsymbol{r}')}}{|\boldsymbol{k}|^{d+\xi}} f(l_\nu|\boldsymbol{k}|) P_{ij}(\boldsymbol{k}) \\
&\quad =: \delta(t-t') d_{ij}(\boldsymbol{r}-\boldsymbol{r}'; l_\nu).
\end{aligned} \tag{1.10}$$

This is all one needs to derive a partial differential equation for the pair correlation function of $\boldsymbol{B}$, but it will still be very difficult to analyze. Hence the approximation, which proceeds as follows:

(1) Consider the asymptotic cases where r is far from the length scales l_κ and l_ν with the separation of the length scales large as well. There are therefore three ranges where the equation is simplified into a much more manageable form. The equations are of the form $\partial_t H - \mathcal{M}H = 0$, where $\mathcal{M}$ is a second order differential operator with respect to the radial variable. We then consider the eigenvalue problem $\mathcal{M}H = zH$.
(2) By a suitable choice of constant parameters in terms of the length scales, we can adjust the differential equations to match in different regions as closely as possible. Solving the equations, we obtain two independent solutions in all ranges.
(3) We match the solutions by requiring continuity and differentiability at the scales l_ν and l_κ. Also appropriate boundary conditions are applied.
(4) According to standard physical lore, the form of cutoffs do not affect the results when the cutoffs are removed. In addition to l_ν, we can interpret l_κ as a cutoff. Therefore we conjecture that the solution approaches the exact one for small cutoffs. We also expect the qualitative results, such as the existence of the dynamo effect, to apply for finite cutoffs as well.

For concreteness, suppose that $\mathcal{M}$ is of the form

$$\mathcal{M} = a(l_\nu, l_\kappa, r)\partial_r^2 + b(l_\nu, l_\kappa, r)\partial_r + c(l_\nu, l_\kappa, r). \tag{1.11}$$

[1] We choose to write the Prandtl number as P instead of the usual Pr since it appears so frequently in formulae.

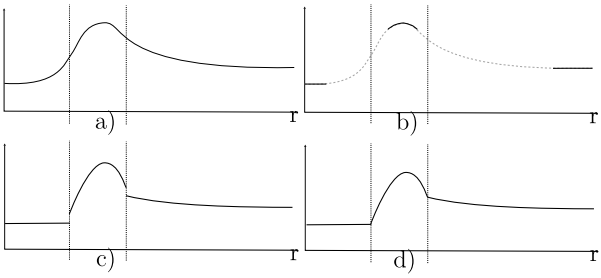

Fig. 1 A sketch of the procedure of approximating the example equation. The *dashed vertical lines* correspond to either one of the length scales l_ν and l_κ with pictures (**a**), a plot of the "real" coefficient, which depends of the cutoff function (and is really unknown), (**b**) an approximate form obtained by taking r far from the length scales (*dotted parts of the lines* are dropped), (**c**) the approximations extended to cover all $r \in \mathbb{R}$, and (**d**) adjusting the coefficients to match at the scales l_ν and l_κ. For r much larger than the cutoffs, the error due to the approximation is lost

The coefficients are some functions of the length scales l_ν and l_κ and the radial variable r. In general, solving the eigenvalue problem for such a differential equation is not possible except numerically. However, we can approximate the coefficients in the asymptotic regions when r is far from the length scales. The asymptotic coefficients are all power laws and solving the equations becomes much easier. Figure 1 illustrates this procedure corresponding to steps (1) and (2) for any of the coefficients.

After some preparations, we begin by writing down the equation for the pair correlation function of the magnetic field using the Itô formula. The derivation can be found in Appendix 1. The equation is of third order in the radial variable, but it can be manipulated into a second order equation by using the incompressibility condition. In Sect. 2 the approximate equations will be derived when $\nu \ll \kappa$ and $\kappa \ll \nu$, or Prandtl number small or large, respectively. We use adimensional variables for sake of convenience and clarity. The focus of the paper is mainly on the existence of the dynamo effect and its growth rate. Therefore we consider the spectrum of $\mathcal{M}$. By a spectral mapping theorem, we relate the spectra of $\mathcal{M}$ and the corresponding semigroup $e^{t\mathcal{M}}$. It is then evident that if the spectrum of $\mathcal{M}$ contains a positive part, there is exponential growth, i.e. a dynamo effect.

1.4 Structure Function Asymptotics

Due to the viscous scale l_ν in the structure function (1.10), there are two extreme scaling ranges $r \gg l_\nu$ (inertial range) and $r \ll l_\nu$. For $r \gg l_\nu$ we can set $l_\nu = 0$ in (1.10) and obtain

$$d_{ij}^{>}(\boldsymbol{r}) := D_1 r^\xi \left((d+\xi-1)\delta_{ij} - \xi \frac{r_i r_j}{r^2} \right), \tag{1.12}$$

where

$$D_1 = \frac{D_0 C_\infty}{(d-1)(d+2)}, \quad C_\infty = \frac{\Gamma(1-\xi/2)}{2^{d+\xi-2}\pi^{d/2}\Gamma(d/2+\xi/2)}. \tag{1.13}$$

The second case corresponds to the viscous range, which is to leading order in r:

$$d_{ij}^{<}(\boldsymbol{r}) := D_2 l_\nu^{\xi-2} r^2 \left((d+1)\delta_{ij} - 2\frac{r_i r_j}{r^2} \right), \tag{1.14}$$

where

$$D_2 = \frac{D_0 C_0}{(d-1)(d+2)}, \quad C_0 = \int đ\boldsymbol{k} \frac{f(k)}{k^{d+\xi-2}}. \tag{1.15}$$

We see that the viscous range form (1.14) can be obtained from (1.12) by a replacement $\xi \to 2$ and $D_1 \to D_2 l_\nu^{\xi-2}$. Note that by adjusting the cutoff function f we can also adjust D_2/D_1.

1.5 Incompressibility Condition

Due to rotation and translation invariance, the equal-time correlation function of $\boldsymbol{B}$ must be of the form

$$G_{ij}(t, |\boldsymbol{x} - \boldsymbol{x}'|) := \langle B_i(t, \boldsymbol{x}) B_j(t, \boldsymbol{x}') \rangle = G_1(t, r)\delta_{ij} + G_2(t, r)\frac{r_i r_j}{r^2}, \tag{1.16}$$

where $r = |\boldsymbol{x} - \boldsymbol{x}'|$. Additional simplification arises from the incompressibility condition $\partial_i G_{ij}(t, r) = 0$:

$$\partial_r G_1(t, r) = -\frac{1}{r^{d-1}} \partial_r (r^{d-1} G_2(t, r)). \tag{1.17}$$

The general solution of the incompressibility condition can be written as

$$\begin{cases} G_1(t, r) = r\partial_r H(t, r) + (d-1)H(t, r), \\ G_2(t, r) = -r\partial_r H(t, r). \end{cases} \tag{1.18}$$

In terms of a so far arbitrary function H. Alternatively, adding the above equations we may write

$$H(t, r) = \frac{1}{d-1} \left(G_1(t, r) + G_2(t, r) \right). \tag{1.19}$$

This observation leads to a considerable simplification in the differential equation for the correlation function: whereas the equations for G_1 and G_2 are of third order in r, we can use the above result to obtain a second order equation for H. Then we would get back to G through (1.18); for example we have for the trace of G:

$$G_{ii}(t, r) = (d-1) \left(r\partial_r H(t, r) + dH(t, r) \right), \tag{1.20}$$

although we refrain from doing this since H has the same spectral properties as G_{ii}.

2 Equations of Motion

The equation of motion for the pair correlation function is derived in Appendix 1:

$$\partial_t G_{ij} = 2\kappa \Delta G_{ij} + d_{\alpha\beta} G_{ij,\alpha\beta} - d_{\alpha j,\beta} G_{i\beta,\alpha} - d_{i\beta,\alpha} G_{\alpha j,\beta} + d_{ij,\alpha\beta} G_{\alpha\beta}. \tag{2.1}$$

The indices after commas are used to denote partial derivatives and we use the Einstein summation. For derivatives with respect to the radial variable r we will simply denote ∂_r. We will also try to avoid writing any arguments, unless it may cause confusion. By taking $r \gg l_\nu$

and $r \ll l_\nu$ we can use the approximations (1.12) and (1.14) to write the equation in the corresponding ranges. This is done for the quantity $H = (G_1 + G_2)/(d-1)$ in Appendix 1 as well, resulting in the equations

$$\partial_t H = \xi(d-1)(d+\xi)D_1 r^{\xi-2}H + \left[2(d+1)\kappa + (d^2-1+2\xi)D_1 r^\xi\right]\frac{1}{r}\partial_r H + \left[2\kappa + (d-1)D_1 r^\xi\right]\partial_r^2 H, \quad r \gg l_\nu, \tag{2.2}$$

and

$$\partial_t H = 2(d-1)(d+2)D_2 l_\nu^{\xi-2}H + \left[2(d+1)\kappa + (d^2+3)D_2 l_\nu^{\xi-2}r^2\right]\frac{1}{r}\partial_r H + \left[2\kappa + (d-1)D_2 l_\nu^{\xi-2}r^2\right]\partial_r^2 H, \quad r \ll l_\nu. \tag{2.3}$$

Simple dimensional analysis leads to the observation

$$[\kappa] = [D_1 r^\xi] = [D_2 l_\nu^{\xi-2} r^2], \tag{2.4}$$

where the brackets denote the scaling dimension of the quantities. We define the length scale l_κ as the scale below which the diffusive effects of κ become important. This will be done explicitly below for different Prandtl number cases. In general, one can write $\kappa = D_1 l_\nu^{\xi-p} l_\kappa^p$ for some $p \in (0, 2]$. Now one just needs to identify the dominant terms in the three scales divided by l_ν and l_κ. For sake of clarity, we choose to write these equations in adimensional variables. This can be done for example by defining $r = l\rho$ and $t = l^{2-\xi}\tau/D_1$ with l being a length scale. It turns out to be convenient to choose the larger of l_κ and l_ν as l. Since we deal with a stochastic velocity field with no intrinsic dynamics, we cannot, in principle, talk about viscosity. However, it is convenient to define a viscosity ν (of dimension length squared divided by time) by dimensional analysis from the length scale l_ν and the dimensional velocity magnitude D_1, giving a relationship between ν, l_ν and D_1 similar to what we would get in a dynamical model. We therefore define

$$\nu := D_1 l_\nu^\xi. \tag{2.5}$$

This permits us to define the Prandtl number in the standard manner as $P = \nu/\kappa$. We then consider the cases $P \ll 1$ and $P \gg 1$.

2.1 Small Prandtl Number

Now $\nu \ll \kappa$, and we choose as adimensional variables

$$\begin{cases} r = l_\kappa \rho, \\ t = \frac{l_\kappa^{2-\xi}}{D_1}\tau. \end{cases} \tag{2.6}$$

Note that the relation between l_κ and κ has not yet been determined. In these variables, (2.2) and (2.3) become

$$\partial_\tau H = \xi(d-1)(d+\xi)\rho^{-2+\xi}H + \left[2(d+1)\frac{\kappa}{D_1 l_\kappa^\xi} + (d^2-1+2\xi)\rho^\xi\right]\frac{1}{\rho}\partial_\rho H + \left[2\frac{\kappa}{D_1 l_\kappa^\xi} + (d-1)\rho^\xi\right]\partial_\rho^2 H, \quad \rho \gg l_\nu/l_\kappa \tag{2.7}$$

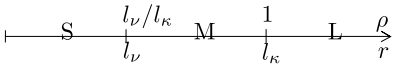

Fig. 2 Sketch of the scaling ranges at small Prandtl number

and

$$\begin{aligned}\partial_\tau H &= 2(d-1)(d+2)\frac{D_2}{D_1}\left(\frac{l_v}{l_\kappa}\right)^{\xi-2} H \\ &+ \left[2(d+1)\frac{\kappa}{D_1 l_\kappa^\xi} + (d^2+3)\frac{D_2}{D_1}\left(\frac{l_v}{l_\kappa}\right)^{\xi-2}\rho^2\right]\frac{1}{\rho}\partial_\rho H \\ &+ \left[2\frac{\kappa}{D_1 l_\kappa^\xi} + (d-1)\frac{D_2}{D_1}\left(\frac{l_v}{l_\kappa}\right)^{\xi-2}\rho^2\right]\partial_\rho^2 H, \quad \rho \ll l_v/l_\kappa. \end{aligned} \tag{2.8}$$

As mentioned above, we also consider $r \ll l_\kappa$ and $r \gg l_\kappa$, that is $\rho \ll 1$ and $\rho \gg 1$, respectively. There are now three regions in ρ, divided by l_v/l_κ and 1, with $l_v/l_\kappa \ll 1$. The regions, solutions and various other quantities will be labelled by S, M and L, corresponding to $\rho \ll l_v/l_\kappa$, $l_v/l_\kappa \ll \rho \ll 1$ and $1 \ll \rho$. See Fig. 2 for quick reference. Therefore the short range equation will be derived from (2.8) and the two others from (2.7). Consider for example explicitly the coefficients of $\partial_\rho^2 H$:

$$\begin{aligned} L:&\quad 2\frac{\kappa}{D_1 l_\kappa^\xi} + (d-1)\rho^\xi, \\ M:&\quad 2\frac{\kappa}{D_1 l_\kappa^\xi} + (d-1)\rho^\xi, \\ S:&\quad 2\frac{\kappa}{D_1 l_\kappa^\xi} + (d-1)\frac{D_2}{D_1}\left(\frac{l_v}{l_\kappa}\right)^{\xi-2}\rho^2. \end{aligned} \tag{2.9}$$

By definition of the length scale l_κ, in the region L the diffusivity is negligible and in the region M it is dominant, as it is in the region S since in there ρ approaches zero. The coefficients are then approximately

$$\begin{aligned} L:&\quad (d-1)\rho^\xi, \\ M:&\quad 2\frac{\kappa}{D_1 l_\kappa^\xi}, \\ S:&\quad 2\frac{\kappa}{D_1 l_\kappa^\xi}. \end{aligned} \tag{2.10}$$

Matching the coefficients of L, M at $\rho = 1$ provides us with a condition (matching between S and M gives nothing new)

$$d - 1 = 2\frac{\kappa}{D_1 l_\kappa^\xi}. \tag{2.11}$$

This is used as a definition of κ as $\kappa = \frac{1}{2}(d-1)D_1 l_\kappa^\xi$. Writing down the short range equation with the above approximations,

$$\partial_\tau H_S = 2(d-1)(d+2)\frac{D_2}{D_1}\left(\frac{l_v}{l_\kappa}\right)^{\xi-2} H_S + (d^2-1)\frac{1}{\rho}\partial_\rho H_S + (d-1)\partial_\rho^2 H_S, \tag{2.12}$$

by using the derived expression for the Prandtl number,

$$P = \frac{\nu}{\kappa} = \frac{2}{d-1}\left(\frac{l_\nu}{l_\kappa}\right)^\xi, \tag{2.13}$$

and by defining

$$\frac{D_2}{D_1} = \left(\frac{2}{d-1}\right)^{1-2/\xi} \tag{2.14}$$

(remember that D_2 could be adjusted by a choice of the cutoff function f, see (1.14) and below) a more neat expression is obtained for the short range equation. We can now write down all the equations:

$$\partial_\tau H_S = 2(d-1)(d+2)P^{1-2/\xi}H_S + (d^2-1)\frac{1}{\rho}\partial_\rho H_S + (d-1)\partial_\rho^2 H_S, \tag{2.15a}$$

$$\partial_\tau H_M = \xi(d-1)(d+\xi)\rho^{-2+\xi}H_M + (d^2-1)\frac{1}{\rho}\partial_\rho H_M + (d-1)\partial_\rho^2 H_M, \tag{2.15b}$$

$$\partial_\tau H_L = \xi(d-1)(d+\xi)\rho^{-2+\xi}H_L + (d^2-1+2\xi)\rho^{\xi-1}\partial_\rho H_L + (d-1)\rho^\xi\partial_\rho^2 H_L. \tag{2.15c}$$

2.2 Large Prandtl Number

Now $\nu \gg \kappa$, and we choose

$$\begin{cases} r = l_\nu \rho, \\ t = \frac{l_\nu^{2-\xi}}{D_1}\tau. \end{cases} \tag{2.16}$$

Then (2.2) and (2.3) for $r \gg l_\nu$ and $r \ll l_\nu$ become in the new variables

$$\partial_\tau H = \xi(d-1)(d+\xi)\rho^{-2+\xi}H + \left[2(d+1)\frac{\kappa}{D_1 l_\nu^\xi} + (d^2-1+2\xi)\rho^\xi\right]\frac{1}{\rho}\partial_\rho H + \left[2\frac{\kappa}{D_1 l_\nu^\xi} + (d-1)\rho^\xi\right]\partial_\rho^2 H, \quad \rho \gg 1 \tag{2.17}$$

and

$$\partial_\tau H = 2(d-1)(d+2)\frac{D_2}{D_1}H + \left[2(d+1)\frac{\kappa}{D_1 l_\nu^\xi} + (d^2+3)\frac{D_2}{D_1}\rho^2\right]\frac{1}{\rho}\partial_\rho H + \left[2\frac{\kappa}{D_1 l_\nu^\xi} + (d-1)\frac{D_2}{D_1}\rho^2\right]\partial_\rho^2 H, \quad \rho \ll 1. \tag{2.18}$$

The ranges S, M and L now correspond to $\rho \ll l_\kappa/l_\nu, l_\kappa/l_\nu \ll \rho \ll 1$ and $1 \ll \rho$, see Fig. 3. Note that equations in both S and M are now derived from (2.18). As before, we consider again the coefficients of $\partial_\rho^2 H$ and drop the terms $\propto \kappa$ in L and $\propto \rho^2$ in S. The diffusive effects are not dominant in the region M since $r \gg l_\kappa$, so we drop the $\propto \kappa$ term in M too.

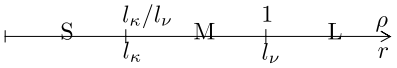

Fig. 3 Sketch of the scaling ranges at large Prandtl number

The approximative coefficients are then

$$\begin{aligned} L:&\quad (d-1)\rho^{\xi},\\ M:&\quad (d-1)\frac{D_2}{D_1}\rho^2,\\ S:&\quad 2\frac{\kappa}{D_1 l_v^{\xi}}. \end{aligned} \tag{2.19}$$

We then obtain two equations by matching the coefficient of L with M at $\rho = 1$ and of M with S at l_κ/l_v:

$$\begin{aligned} &\frac{D_2}{D_1}(d-1) = (d-1),\\ &(d-1)\frac{D_2}{D_1}\left(\frac{l_\kappa}{l_v}\right)^2 = 2\frac{\kappa}{D_1 l_v^{\xi}}, \end{aligned} \tag{2.20}$$

with solutions

$$\begin{aligned} &D_2 = D_1,\\ &\kappa = \frac{d-1}{2} D_1 l_\kappa^2 l_v^{\xi-2}. \end{aligned} \tag{2.21}$$

The Prandtl number is in this case

$$P = \frac{2}{d-1}\left(\frac{l_v}{l_\kappa}\right)^2. \tag{2.22}$$

Note that one can obtain this from the small Prandtl number equation (2.13) by replacing $\xi \to 2$. This is a reflection of a more subtle observation that the large Prandtl number case for *any* ξ is similar to the small Prandtl number case with $\xi = 2$. We collect the equations using the above approximations,

$$\partial_\tau H_S = 2(d-1)(d+2)H_S + 2\frac{d+1}{P}\frac{1}{\rho}\partial_\rho H_S + \frac{2}{P}\partial_\rho^2 H_S, \tag{2.23a}$$

$$\partial_\tau H_M = 2(d-1)(d+2)H_M + (d^2+3)\rho\partial_\rho H_M + (d-1)\rho^2\partial_\rho^2 H_M, \tag{2.23b}$$

$$\partial_\tau H_L = \xi(d-1)(d+\xi)\rho^{-2+\xi}H_L + (d^2-1+2\xi)\rho^{\xi-1}\partial_\rho H_L + (d-1)\rho^{\xi}\partial_\rho^2 H_L. \tag{2.23c}$$

Note that the short and long range equations are somewhat similar to the respective small Prandtl number ones, (2.15a) and (2.15c). However, the equation in the medium range above is scale invariant in ρ, unlike the corresponding small Prandtl number one (2.15b).

3 Resolvent

In the preceding section we have reduced the evolution of the two-point function of the magnetic field to a parabolic partial differential equation (PDE) of the form $\partial_\tau H = \mathcal{M}H$, where $\mathcal{M}$ is an elliptic operator on the positive half-line.

We are now concerned with finding the fastest possible long time asymptotic growth rate of a solution H. If that maximal growth rate is positive then we say that there is dynamo effect with that growth rate.

In mathematical terminology, the operator $\mathcal{M}$ is the generator of a time evolution semigroup acting on (the space of the) H and the maximum growth rate is the maximum real part of the spectrum of the evolution semigroup. We expose below how the spectrum of the semigroup is related to that of its generator, and then study the spectrum of $\mathcal{M}$.

3.1 General Considerations

Given a differential operator $\mathcal{M}$ with a domain $D(\mathcal{M})$, we define the resolvent

$$R(z, \mathcal{M}) := (z - \mathcal{M})^{-1} \tag{3.1}$$

and the resolvent set as

$$\varrho(\mathcal{M}) := \{z \in \mathbb{C} | z - \mathcal{M} : D(\mathcal{M}) \to \mathrm{X} \text{ is bijective}\}. \tag{3.2}$$

The complement of the resolvent set, denoted by $\sigma(\mathcal{M})$, is the spectrum of $\mathcal{M}$.

According to the well known Hille-Yosida theorems (see e.g. [7]), if $(\mathcal{M}, D(\mathcal{M}))$ is closed and densely defined and if there exists $z_0 \in \mathbb{R}$ such that for each $z \in \mathbb{C}$ with $\Re z > z_0$ we have $z \in \varrho(\mathcal{M})$, and additionally the resolvent estimate $\|R(z, \mathcal{M})\| \leq 1/(\Re z - z_0)$ holds, then $\mathcal{M}$ is the generator of a strongly continuous semigroup $T(t)$ satisfying $\|T(t)\| \leq e^{z_0 t}$. However the last inequality gives only an upper bound on the growth rate of the semigroup, and this bound is not necessarily strict, so it is not possible to say exactly how fast grows the norm of the vector which is fastest stretched under the action of the semigroup.

Therefore we shall need in our analysis the somewhat stronger property of spectral mapping, relating the spectrum of the generator to that of the semigroup:

$$\sigma(T(t)) = \{0\} \cup e^{t\sigma(\mathcal{M})}. \tag{3.3}$$

This is the case in particular if $\mathcal{M}$ is a so called sectorial operator, meaning that its spectrum is contained in some angular sector $\{z \in \mathbb{C} : |\arg(z - z_0)| > \alpha > \pi/2\}$ and that outside this sector the resolvent satisfies the (stronger) estimate

$$\|R(z, \mathcal{M})\| \leq \frac{C}{|z - z_0|}. \tag{3.4}$$

Under these hypotheses $\mathcal{M}$ generates an analytic semigroup, for which the spectral mapping property (3.3) holds.

We take a moment to remind the reader that analytic semigroups are those to which physicists are used, for example one can use for them the Cauchy integral formula:

$$T(t) := e^{t\mathcal{M}} = \frac{1}{2\pi i} \int_{\mathcal{C}} dz e^{zt} R(z, \mathcal{M}), \tag{3.5}$$

where the contour surrounds the spectrum $\sigma(\mathcal{M})$. However all strongly continuous semigroups are not analytic.

We do not prove in the present work that $\mathcal{M}$ is sectorial, however we refer the interested reader to the general mathematical theory in [19] where it is explained and substantiated

that strongly elliptic operators are, under quite general assumption, sectorial generators, on a wide range of Banach spaces (e.g. L^p and C^1 spaces to name but a few).

According to the above discussion, in order to explain the existence of the dynamo effect and its growth rate, we only need to find the spectrum of $\mathcal{M}$ via the resolvent set $\varrho(\mathcal{M})$. Note that we are interested only in the positive part of the spectrum, since we want to determine the existence of the dynamo effect only.

3.2 The Resolvent Equations

The operator $\mathcal{M}$ in our case is cut up as the operators $\mathcal{M}_L$, $\mathcal{M}_M$ and $\mathcal{M}_S$ in the corresponding ranges, obtained from (2.15a) and (2.23). The resolvent is found from the equation

$$(z - \mathcal{M})\, R(z, \mathcal{M})(\rho, \rho') = \delta(\rho - \rho'). \tag{3.6}$$

Since we are primarily interested in the long range (L) behavior $\rho > 1$, we let ρ' stay in the region L at all times. This results in three equations

$$\begin{cases} (z - \mathcal{M}_L)\, R_L(\rho, \rho') = \delta(\rho - \rho'), \\ (z - \mathcal{M}_M)\, R_M(\rho, \rho') = 0, \\ (z - \mathcal{M}_S)\, R_S(\rho, \rho') = 0, \end{cases} \tag{3.7}$$

where $R_L(\rho, \rho')$ is the expression of the resolvent for $\rho \in L$ (the large scale range) and $\rho' \in \mathbb{R}_+$ and similarly R_M and R_S are valid when ρ is in the middle and small scale ranges respectively. We require the following boundary conditions from the resolvents: for small ρ we are in the diffusion dominated range, so we require smooth behavior at $\rho \to 0$. For large ρ we eventually cross the integral scale (although we haven't defined it explicitly) above which the velocity field behaves like the $\xi = 0$ Kraichnan model, leading to diffusive behavior at the largest scales for which the appropriate condition on the resolvent is exponential decay at infinity.

3.3 Piecewise Solutions of the Resolvent Equations

Assuming $\rho \neq \rho'$, we solve (3.7) with the corresponding operators $\mathcal{M}$.

The operator $\mathcal{M}_L$ does not depend on the Prandtl number. So in the region L, we get from e.g. (2.23c) (we use lowercase letters $h^{\pm}$ to denote the independent solutions)

$$h_L^{\pm}(\rho) = \rho^{-d/2 - \frac{\xi}{d-1}}\, \tilde{Z}_\lambda^{\pm}(w\rho^{1-\xi/2}), \tag{3.8}$$

where $\tilde{Z}_\lambda^{+} \equiv I_\lambda$ and $\tilde{Z}_\lambda^{-} \equiv K_\lambda$ are modified Bessel functions of the first and second kind respectively, and we have introduced w related to z by

$$w = \frac{2}{2-\xi}\sqrt{\frac{z}{(d-1)}} \quad \text{and} \quad z = (d-1)\left(\frac{2-\xi}{2}w\right)^2, \tag{3.9}$$

and the order parameter λ is

$$\lambda = \frac{\sqrt{d[2(d-1)^3 - (d-2)(2\xi + d - 1)^2]}}{(2-\xi)(d-1)}. \tag{3.10}$$

Because the range S is always in the diffusive region, we require smoothness of the solution at zero. Only one of the solutions satisfies this, so we get from (2.15a) and (2.23a)

$$h_{S,1}(\rho) = \rho^{-d/2}\, I_{d/2}\left(\sqrt{\frac{z}{d-1} - 2(d+2)P^{1-2/\xi}}\,\rho\right) \tag{3.11}$$

and

$$h_{S,2}(\rho) = \rho^{-d/2}\, I_{d/2}\left(\sqrt{\frac{z}{2} - (d-1)(d+2)\sqrt{P}}\;\rho\right), \tag{3.12}$$

where the subindex 1 refers to $P \ll 1$ (small Prandtl number) and 2 to $P \gg 1$. We will use this notation in other objects as well.

In the range M, when $P \gg 1$ we have the scale invariant equation in (2.23b) with power law solutions

$$h^{\pm}_{M,2}(\rho) = \rho^{-d/2-\frac{2}{d-1}\pm\zeta}, \tag{3.13}$$

where

$$\zeta = \sqrt{\frac{z - z_2}{d-1}}, \tag{3.14}$$

with

$$z_2 = -\frac{d-1}{4}[(2-\xi)\lambda]^2|_{\xi=2} = -\frac{d}{4(d-1)}(d^3 - 10d^2 + 9d + 16). \tag{3.15}$$

The medium range equation for $P \ll 1$ cannot be solved exactly, but we can consider it in two different asymptotic cases. From (2.15b) we get

$$\left(\xi(d+\xi)\rho^{-2+\xi} - \frac{z}{d-1}\right) R_M + (d+1)\frac{1}{\rho}\partial_\rho R_M + \partial^2_\rho R_M = 0 \tag{3.16}$$

and note that since by definition of the medium range $l_v/l_\kappa \ll \rho \ll 1$, implying $1 < \rho^{-2+\xi} < (l_\kappa/l_v)^{2-\xi}$ (the $\ll$ was replaced by $<$, so that things remain valid even as $\xi \to 2$), the term $\propto \rho^{-2+\xi}$ can be dropped if we assume that

$$|z| \gg (l_\kappa/l_v)^{2-\xi} \approx P^{-\frac{2-\xi}{\xi}}. \tag{3.17}$$

If on the other hand we have

$$|z| \ll 1, \tag{3.18}$$

then z can be neglected in the equation.

The solution for large z is similar to the short range solutions,

$$h^{\pm}_{M,1}(\rho) = \rho^{-d/2}\tilde{Z}^{\pm}_{d/2}\left(\sqrt{\frac{z}{d-1}}\rho\right), \quad |z| \gg (l_\kappa/l_v)^{2-\xi}, \tag{3.19}$$

where we denoted the $P \ll 1$ case by a subscript 1. For small z we have instead

$$h^{\pm}_{M,1} = \rho^{-d/2} Z^{\pm}_{d/\xi}(2\sqrt{d/\xi + 1}\rho^{\xi/2}), \quad |z| \ll 1, \tag{3.20}$$

where $Z^+_{d/\xi} \equiv J_{d/\xi}$ and $Z^-_{d/\xi} \equiv Y_{d/\xi}$ are Bessel functions of the first and second kind respectively. It turns out however that the explicit form of the above solutions affects only a specific numerical multiplier and has no effect on the presence of the dynamo. Because of this we in fact derive a lower bound for the growth rate which in view of the present approximation provides a more reliable result.

3.4 Matching of the Solutions

Consider equations (3.7). We denote the long range regions $\rho < \rho'$ and $\rho > \rho'$ as $L_<$ and $L_>$. The boundary conditions for the resolvent demanded finiteness at $\rho = 0$, but in general the resolvent must be in $L_2(\mathbb{R}_+)$. We therefore have in the region $L_>$ only the h^-_L solution, since it decays as a stretched exponential at infinity (the other one grows as a stretched exponential). We also drop the subscripts labelling the different Prandtl number cases for now. The full solutions are written as follows:

$$\begin{cases} R_S(z|\rho,\rho') = \alpha h_S(\rho), \\ R_M(z|\rho,\rho') = C^+_M h^+_M(\rho) + C^-_M h^-_M(\rho), \\ R_{L_<}(z|\rho,\rho') = C^+_L h^+_L(\rho) + C^-_L h^-_L(\rho), \\ R_{L_>}(z|\rho,\rho') = \beta h^-_L(\rho). \end{cases} \tag{3.21}$$

We denote the matching point between the short and medium ranges by a_i, i.e.

$$\begin{cases} a_1 = l_v/l_\kappa, \\ a_2 = l_\kappa/l_v. \end{cases} \tag{3.22}$$

The other matching points are $\rho = 1$ and $\rho = \rho'$ in both cases. There are six coefficients to be determined, $\alpha, C^\pm_M, C^\pm_L$ and β, and in total six conditions, four from the continuity and differentiability at $\rho = a_i$ and $\rho = 1$ and two conditions at $\rho = \rho'$ around the delta function, so all coefficients will be determined from these. They will then depend on the variables z and ρ'. The C^1 conditions at $\rho = 1$ are

$$C^+_L h^+_L + C^-_L h^-_L(1) = C^+_M h^+_M(1) + C^-_M h^-_M(1) \tag{3.23}$$

and

$$C^+_L \partial h^+_L(1) + C^-_L \partial h^-_L(1) = C^+_M \partial h^+_M(1) + C^-_M \partial h^-_M(1), \tag{3.24}$$

where we denoted $\partial h(1) = \partial_\rho h(\rho)|_{\rho=1}$. This can be expressed conveniently as

$$\begin{pmatrix} h^+_L & h^-_L \\ \partial h^+_L & \partial h^-_L \end{pmatrix}_1 \begin{pmatrix} C^+_L \\ C^-_L \end{pmatrix} = \begin{pmatrix} h^+_M & h^-_M \\ \partial h^+_M & \partial h^-_M \end{pmatrix}_1 \begin{pmatrix} C^+_M \\ C^-_M \end{pmatrix}, \tag{3.25}$$

where the matrix subindex refers to evaluation of the matrix elements at $\rho = 1$. Since we have only one solution at short range, we get similarly at a_i

$$\begin{pmatrix} h^+_M & h^-_M \\ \partial h^+_M & \partial h^-_M \end{pmatrix}_{a_i} \begin{pmatrix} C^+_M \\ C^-_M \end{pmatrix} = \alpha \begin{pmatrix} h_S \\ \partial h_S \end{pmatrix}_{a_i}, \tag{3.26}$$

where again the matrix subindex indicates the point where matrix elements are to be evaluated. We can solve these for $C^\pm_L$,

$$\begin{pmatrix} C^+_L \\ C^-_L \end{pmatrix} = \mathcal{J}' \begin{pmatrix} \partial h^-_L & -h^-_L \\ -\partial h^+_L & h^+_L \end{pmatrix}_1 \begin{pmatrix} h^+_M & h^-_M \\ \partial h^+_M & \partial h^-_M \end{pmatrix}_1 \begin{pmatrix} \partial h^-_M & -h^-_M \\ -\partial h^+_M & h^+_M \end{pmatrix}_{a_i} \begin{pmatrix} h_S \\ \partial h_S \end{pmatrix}_{a_i}. \tag{3.27}$$

The numeric constant $\mathcal{J}'$ above contains the determinants of the inverted matrices and α. It is certainly nonsingular due to the linear independence of the solutions. We have decided not to explicitly write it down since, as we will see below, we only need the fraction C_L^-/C_L^+. Now we have piecewise the resolvents

$$\begin{cases} R_{L_<}(z|\rho,\rho') = C_L^+(h_L^+(\rho) + \frac{C_L^-}{C_L^+}h_L^-(\rho)), \\ R_{L_>}(z|\rho,\rho') = \beta h_L^-(\rho), \end{cases} \tag{3.28}$$

and we still need to use the first equation of (3.7) for C_L^+ and β. The continuity condition is

$$C_L^+\left(h_L^+(z,\rho') + \frac{C_L^-}{C_L^+}h_L^-(z,\rho')\right) = \beta h_L^-(z,\rho'). \tag{3.29}$$

The other condition is obtained by integrating the equation with respect to ρ over a small interval and then shrinking the interval to zero:

$$C_L^+\left(\partial h_L^+(\rho') + \frac{C_L^-}{C_L^+}\partial h_L^-(\rho')\right) - \beta\partial h_L^-(\rho') = 1. \tag{3.30}$$

These can be solved to yield

$$C_L^+ = \frac{h_L^-(\rho')}{\mathcal{W}(h_L^+,h_L^-)(\rho')} \tag{3.31}$$

and

$$\beta = \frac{C_L^+h_L^+(\rho') + C_L^-h_L^-(\rho')}{C_L^+\mathcal{W}(h_L^+,h_L^-)(\rho')}, \tag{3.32}$$

where $\mathcal{W}$ is the Wronskian, $\mathcal{W}(f,g) = fg' - f'g$. Explicitly from (3.8),

$$\mathcal{W}(h_L^+,h_L^-)(z,\rho') = (\rho')^{-d-\frac{2\xi}{d-1}}\mathcal{W}(I_\lambda,K_\lambda) = -(1-\xi/2)(\rho')^{-d-1-\frac{2\xi}{d-1}}. \tag{3.33}$$

Using the above obtained expressions of C_L^+, β and $\mathcal{W}$ in (3.28) we thus have the solutions

$$\begin{cases} R_{L_<}(z|\rho,\rho') = -\frac{(\rho')^{d+1+2\xi/(d-1)}}{1-\xi/2}(h_L^+(\rho)h_L^-(\rho') + (\frac{C_L^-}{C_L^+})h_L^-(\rho)h_L^-(\rho')), \\ R_{L_>}(z|\rho,\rho') = -\frac{(\rho')^{d+1+2\xi/(d-1)}}{1-\xi/2}(h_L^-(\rho)h_L^+(\rho') + (\frac{C_L^-}{C_L^+})h_L^-(\rho)h_L^-(\rho')), \end{cases} \tag{3.34}$$

with C_L^-/C_L^+ obtained from (3.27). We have calculated in Appendix 2 the asymptotic expression for C_L^-/C_L^+ for the two Prandtl number cases $P \ll 1$ and $P \gg 1$,

$$\frac{C_L^-}{C_L^+} = -\frac{\partial h_L^+(1) - \Lambda_L h_L^+(1)}{\partial h_L^-(1) - \Lambda_L h_L^-(1)}, \tag{3.35}$$

with leading order contribution to Λ_L as

$$\Lambda_L = \frac{\partial h_M^\pm(1)}{h_M^\pm(1)}, \tag{3.36}$$

with either the $+$ or the $-$ solution understood, the choice depending on the Prandtl number.

4 Dynamo Effect

The mean field dynamo effect for the 2-point function of the magnetic field corresponds to the case when the evolution operator $\mathcal{M}$ has positive (possibly generalized) eigenvalues. Eigenvalues correspond to poles, in z, of the resolvent given in (3.34) and generalized eigenvalues to branch cuts. The z dependence is not seen explicitly in (3.34), but recall from (3.8) that the $h_L^{\pm}$ depend on z, and we see from (3.35) and matter in Appendix 2 that there is further dependence through C_L^-/C_L^+.

The $h_L^{\pm}$ (see (3.8)) depend on the square root of z, and since the Bessel functions are analytic on the complex right half-plane, this square root dependence leads directly to a branch cut along the negative real axis in the z dependence of the resolvent. This corresponds to a heat equation like continuum spectrum of decaying modes, these modes don't contribute to the dynamo effect.

Any other possible contributions to the spectrum come from the fraction C_L^-/C_L^+. An expression for the latter is given in (3.35), with Λ_L computed in Appendix 2. Equation (3.35) can be simplified by noting that (using (3.8) and (3.9))

$$\partial h_L^{\pm}(1) = -\left(\frac{d}{2} + \frac{\xi}{d-1}\right)\tilde{Z}_\lambda^{\pm}(w) + (1-\xi/2)\partial_w \tilde{Z}_\lambda^{\pm}(w). \tag{4.1}$$

Then we can write

$$\frac{C_L^-}{C_L^+} = -\frac{(1-\xi/2)wI_\lambda'(w) - [\frac{d}{2} + \frac{\xi}{d-1} + \Lambda_L]I_\lambda(w)}{(1-\xi/2)wK_\lambda'(w) - [\frac{d}{2} + \frac{\xi}{d-1} + \Lambda_L]K_\lambda(w)}\,. \tag{4.2}$$

We underline again that w depends on the square root of z, so the complex plane minus the negative real line for z corresponds to the $\Re w > 0$ half-plane for w. Since Bessel functions are analytical on this half-plane, the new singularities introduced by C_L^-/C_L^+ may come either from singularities of Λ_L or zeros of the denominator C_L^+. Let us introduce

$$\tilde{\Lambda}_L = \frac{2}{2-\xi}\left[\frac{d}{2} + \frac{\xi}{d-1} + \Lambda_L\right]. \tag{4.3}$$

Then the condition $C_L^+ = 0$ may be written

$$w\frac{K_\lambda'(w)}{K_\lambda(w)} = \tilde{\Lambda}_L. \tag{4.4}$$

Finally we remind the reader that z corresponds to the growth rate with respect to the reduced time τ rather than real time t, and the real growth rate is thus $(\tau/t)z$, where for the $P \to 0$ case from (2.6) we have $\tau/t = D_1 l_\kappa^{\xi-2}$ and for the $P \to \infty$ case from (2.16) we have $\tau/t = D_1 l_\nu^{\xi-2}$.

4.1 Prandtl Number $P \to 0$

In Appendix 3.1.2 it is shown that Λ_L does not introduce new singularities in the small Prandtl case, so we only need to solve in w (4.4). In particular we are interested in the largest solution of that equation, since that will give the growth rate of the fastest growing mode of the two-point function of the magnetic field, and that is what we call the dynamo growth rate. In this aim we first study the large and small w asymptotics of the two sides of (4.4) and then, based on that, we derive estimates for its largest solution.

4.1.1 Asymptotics of $\tilde{\Lambda}_L$

As shown in Appendix 2.1, (8.18), in the limit of vanishing Prandtl number and for large z,—or equivalently large w,—from the medium range solutions of (3.19) we get

$$\Lambda_L = (1-\xi/2)w\frac{I_{1+d/2}((1-\xi/2)w)}{I_{d/2}((1-\xi/2)w)}. \tag{4.5}$$

For large w we deduce from the asymptotic properties of Bessel functions [13] that $\Lambda_L \sim (1-\xi/2)w$.

As shown in Appendix 2.1, (8.21), in the limit of vanishing Prandtl number and for small z,—or equivalently small w,—from the medium range solutions of (3.20) we get

$$\Lambda_L = -\xi\sqrt{d/\xi+1}\frac{J_{d/\xi+1}(2\sqrt{d/\xi+1})}{J_{d/\xi}(2\sqrt{d/\xi+1})}, \tag{4.6}$$

which is obviously independent of w, so it is in fact the $w \to 0$ limit of Λ_L, which we shall denote by $\Lambda_L(0)$.

4.1.2 Asymptotics of $wK'_\lambda(w)/K_\lambda(w)$

From the asymptotic properties of Bessel functions [13] we deduce that, when w goes to infinity, $K'_\lambda(w)/K_\lambda(w) \sim -w$.

However, except for the above large w asymptotics, the behaviour of $wK'_\lambda(w)/K_\lambda(w)$ is very different according to weather λ is real or pure imaginary. Based on its definition in (3.10), λ is pure imaginary if

$$\xi > \xi^* := (d-1)\left(\sqrt{\frac{d-1}{2(d-2)}} - \frac{1}{2}\right) \tag{4.7}$$

and it is real otherwise, and indeed positive (possibly infinite) since we take $\xi \leq 2$ and $d \geq 1$. We study separately the two cases below.

Pure Imaginary λ For λ pure imaginary, $K_\lambda(w)$ has an infinity of positive zeros (may be seen from its small w development), accumulating at $w = 0$, and $wK'_\lambda(w)/K_\lambda(w)$ has a pole at each of those zeros. Importantly for us, $K_\lambda(w)$ has a largest positive zero (may be seen from its large w asymptotics), which we shall denote by w_0.

Since for large w, asymptotically $K_\lambda(w) \sim (\pi/2w)^{1/2}\exp(-w) > 0$, we must have $K'_\lambda(w_0) > 0$ (note that we can exclude $K_\lambda(w_0) = K'_\lambda(w_0) = 0$, since the Bessel function is the solution of a second order homogeneous differential equation). Hence the pole of $wK'_\lambda(w)/K_\lambda(w)$ at w_0 has a positive coefficient.

Real Positive λ Using the integral representation of the modified Bessel function of the second kind,

$$K_\lambda(w) = \int_0^\infty dt e^{-w\cosh(t)}\cosh(\lambda t), \tag{4.8}$$

we see that when $\lambda \in \mathbb{R}$ and $w > 0$, then $K_\lambda(w) > 0$.

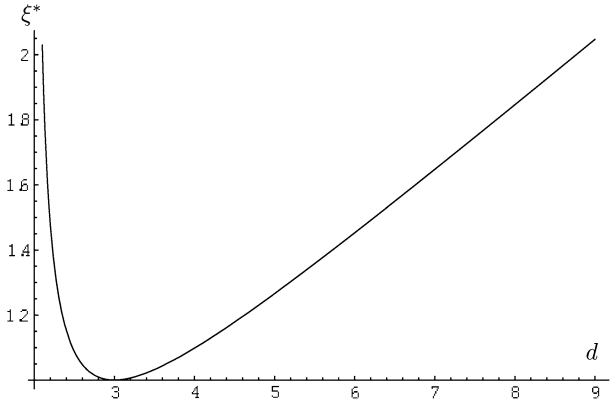

Fig. 4 Plot of the critical value ξ^* as a function of d

On the other hand using the recurrence relation $K'_\lambda(w) = -K_{\lambda-1}(w) - \lambda K_\lambda(w)/w$ we get $wK'_\lambda(w)/K_\lambda(w) = -\lambda - wK_{\lambda-1}(w)/K_\lambda(w)$, and since $K_\lambda(w)$ and $K_{\lambda-1}(w)$ are both positive, we deduce

$$w\frac{K'_\lambda(w)}{K_\lambda(w)} \leq -\lambda. \tag{4.9}$$

Using the power series development of Bessel functions we also get that $wK'_\lambda(w)/K_\lambda(w) \to -\lambda$ as $w \to 0$.

4.1.3 Presence of Dynamo at $\xi > \xi^*$ and Bounds on Growth Rate

We are now going to use the above characterized asymptotic behaviours of the two side of (4.4) to derive estimates on its largest solution. We start with the case of ξ above the critical value ξ^*, which is equivalent to λ being pure imaginary. Note that since $\xi \leq 2$ necessarily, this case is only meaningful if $\xi^* < 2$, which we shall suppose here. The plot in Fig. 4 shows that this is the case for $d_{\min} < d < d_{\max}$, with $d_{\min} \approx 2.1$ and $d_{\max} \approx 8.8$.

Lower Bound We have shown above that for large w the l.h.s. of (4.4) behaves as $-w$ while the r.h.s. behaves as $(1 - \xi/2)w$, furthermore that the l.h.s. has a rightmost pole at $w_0 > 0$ and that this pole has a positive coefficient. Using continuity of the two sides we deduce—see also Fig. 5—that (4.4) admits a solution which is larger than w_0. Hence, there is a dynamo and its growth rate is bounded from below by $z(w_0)$ (cf. (3.9) for the relation between z and w).

One can also obtain upper bounds on the dynamo growth rate. Of course we hope to find one of the same order of magnitude as the lower bound w_0, so that we could use w_0 not just a lower bound but as a convenient estimate of the largest solution of (4.4). We show below the existence of such an upper bound near $\xi = \xi^*$ and near $\xi = 2$, without succeeding to do this for intermediate values of ξ.

We still believe that w_0 is not just a lower bound for the dynamo growth rate but in fact a rather good *estimate* of it. To corroborate this claim, we have plotted in Fig. 6 the value of w_0 as a function of ξ for the $d = 3$ dimensional case, and it indeed compares well with the numerical results for the dynamo growth rate obtained in [23]. The agreement is all the more remarkable that the numerical results are based on the exact evolution equation for the two-point function of the magnetic field, whereas we started our analysis by deriving the approximating system (2.15).

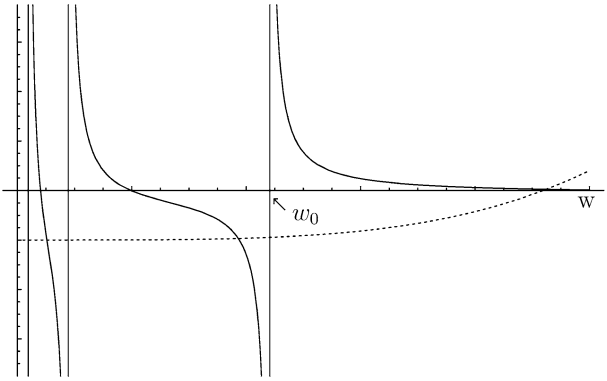

Fig. 5 Based on the asymptotic properties of the left and right hand sides of (4.4), when λ is pure imaginary and $K_\lambda(w)$ has a largest zero w_0, the latter has to be a lower bound on the largest solution of (4.4). The *dashed line* depicts the right hand side of the equation and the *solid line* the left hand side

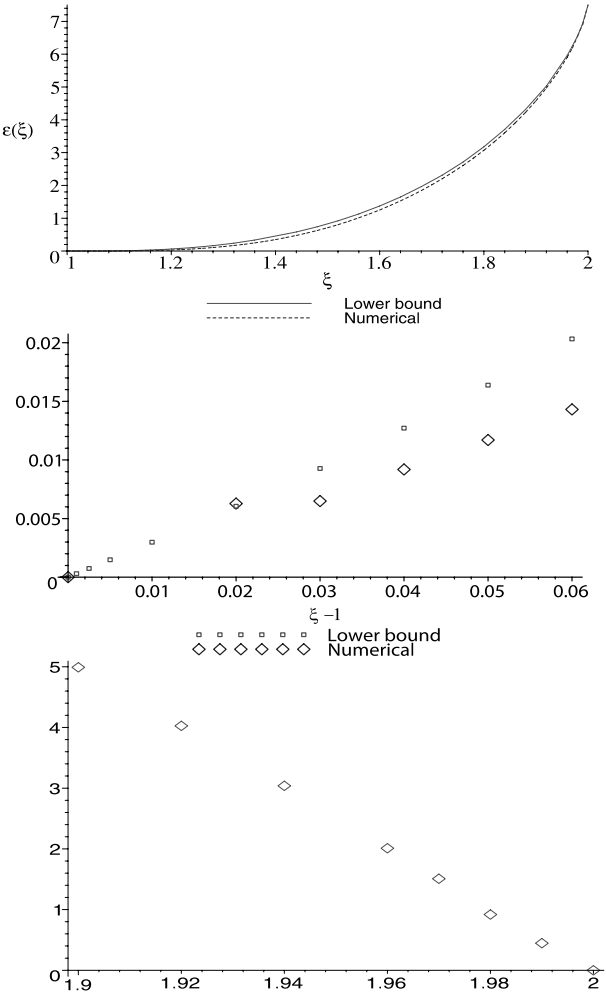

Fig. 6 In the above figure we have plotted the lower bound w_0 with the numerical results of [23]. The middle figure shows plots of both data with $1/\log(\epsilon(\xi))^2$ on the y-axis. The lower bound data shows linear behavior consistent with the asymptotics in (4.12). We note that there seems to be a numerical error in the data of [23] for $\xi = 1.02$. In the *lowest figure* we have also plotted the numerical data in [23] near $\xi = 2$ for $(15/2 - \epsilon(\xi))^{3/2}$ showing linear behavior as expected in (4.13). The plots in other dimensions look similar, except that they begin from the critical value $\xi^* > 1$

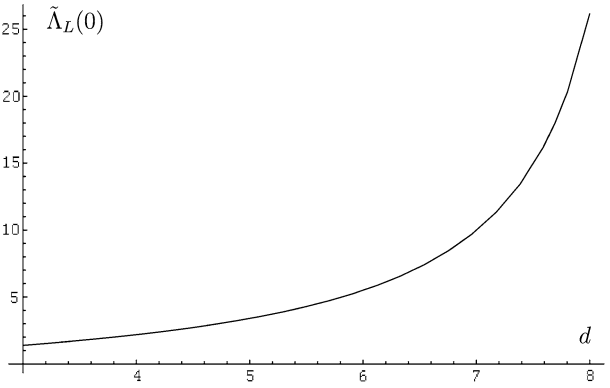

Fig. 7 Plot of $\tilde{\Lambda}_L(0)$ as a function of $\xi^*(d)$ with d taking values between 3 and 8

Upper Bound First we note that, as shown in Appendix 3.1.2, Λ_L is increasing. The small w (equivalently, small z) asymptotics of Λ_L is given in (4.6). It will be now convenient to write out explicitly the dependence of $\tilde{\Lambda}_L$ on w, by employing the notation $\tilde{\Lambda}_L(w)$. The special case $\tilde{\Lambda}_L(0)$ is taken to mean the $w \to 0$ limit of $\tilde{\Lambda}_L(w)$, and this is coherent with the previous use of the symbol.

Two cases are distinguished, depending on the sign of $\tilde{\Lambda}_L(0)$. If $\tilde{\Lambda}_L(0) \geq 0$, then we have the upper bound w_0', where w_0' is the largest zero of K_λ'. This is a good upper bound in the sense that it is always of the same order as the lower bound w_0.

In the contrary case of $\tilde{\Lambda}_L(0) < 0$ we use $\partial_w(wK_\lambda'(w)/K_\lambda(w)) < -1$ from Appendix 3.2 and get the upper bound $w_1 = w_0' + |\tilde{\Lambda}_L(0)|$. However, this upper bound is not as good as just w_0', because it cannot be directly compared to the lower bound w_0.

The asymptotic estimates computed in Sect. 4.1.5 rely on the stronger upper bound w_0', at least for ξ in some neighbourhood of ξ^* and 2 respectively.

For $\xi = \xi^*$ we have $\tilde{\Lambda}_L(0) > 0$, as shown in Fig. 7, where $\tilde{\Lambda}_L$ comes from (4.3) and $\Lambda_L(0)$ is taken from (4.6). By continuity, we still have $\tilde{\Lambda}_L(0) > 0$ on some neighbourhood of ξ^*, and by the above w_0' is a valid upper bound there.

The situation for the $\xi \to 2$ asymptotics is more complicated but in Appendix 2.1.3 it is explained why near $\xi = 2$ we may use the upper bound w_0': although $\tilde{\Lambda}_L(0) < 0$, we can justify $\tilde{\Lambda}_L(w) > 0$ for w corresponding to the dynamo growth rate.

4.1.4 Absence of Dynamo at $\xi \leq \xi^*$

So far we have dealt with the case when $\xi^* < \xi \leq 2$, and we were able to show the existence of a dynamo effect and give bounds for the dynamo growth rate. We are now going to argue that in all other situations there is no dynamo effect. Note that the absence of dynamo for $\xi \leq \xi^*$ (i.e. λ real) can be shown outside of our approximation scheme (2.15), as shown in Appendix 4. Here we show that the absence of dynamo for $\xi \leq \xi^*$ holds also for the approximate system (though much less obviously), thus further validating the scheme.

First we study the case of $d \geq 3$ and distinguish two situations. For $3 \leq d \leq 8$ the critical ξ^* takes values between 1 and 2, in particular for $d = 3$ we get $\xi^* = 1$ as expected [15, 22, 23]. For $d \geq 9$ we get $\xi^* > 2$ so necessarily $\xi < \xi^*$ since $\xi \leq 2$. We are going to show below that for ξ such that

$$0 \leq \xi \leq \min(\xi^*, 2), \tag{4.10}$$

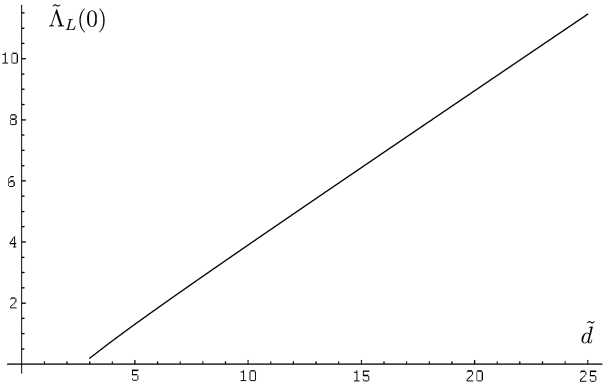

Fig. 8 Plot of the bracketed part of $\tilde{\Lambda}_L(0)$ as a function of $\tilde{d} \in (3 \ldots 25)$

we have $\tilde{\Lambda}_L(0) > 0$, whence (recall that $\tilde{\Lambda}_L(w)$ increases with w) the r.h.s. of (4.4) is always positive. On the other hand for the l.h.s. of (4.4) we have the estimate (4.9). Hence there can be no solutions of (4.4), hence no dynamo.

To prove $\tilde{\Lambda}_L(0) > 0$ as claimed above, we first write, based on (4.4), the estimate

$$\tilde{\Lambda}_L \geq \frac{2\xi}{2-\xi}\left[\frac{d}{2\xi} + \frac{\Lambda_L}{\xi}\right].$$

In particular for $w = 0$ one may use the value of $\Lambda_L(0)$ from (4.6). Using the parameter $\tilde{d} = d/\xi$, we can write then

$$\tilde{\Lambda}_L(0) \geq \frac{2\xi}{2-\xi}\left[\frac{\tilde{d}}{2} - \sqrt{\tilde{d}+1}\,\frac{J_{\tilde{d}+1}(2\sqrt{\tilde{d}+1})}{J_{\tilde{d}}(2\sqrt{\tilde{d}+1})}\right]. \tag{4.11}$$

From (4.10) and $d \geq 3$ we have $\tilde{d} \geq d/\min(\xi^*, 2)$, and using additionally (4.7) we may obtain $\tilde{d} \geq 3$. Now a plot in Fig. 8 of the term inside brackets in (4.11) and the fact that asymptotically the bracketed term behaves as $\tilde{d}/2 - \sqrt{\tilde{d}/2+1}$ can convince us that it is positive for $\tilde{d} \geq 3$, and hence that $\tilde{\Lambda}_L(0) > 0$ as claimed.

For $d = 2$ one readily verifies that $\xi^* = +\infty$, so necessarily $\xi < \xi^*$ since $\xi \leq 2$. We may again use the estimate (4.9) for the l.h.s. of (4.4), however the r.h.s. is not anymore positive. But the plot in Fig. 9 shows that $\tilde{\Lambda}_L(0) > -\lambda$ and we have shown that $\tilde{\Lambda}_L(w)$ grows with w. This excludes the presence of solutions to (4.4).

We have thus found that in dimensions $3 \leq d \leq 8$ a critical value $1 \leq \xi^* < 2$ exists above which the dynamo is present and below which we don't expect it to be present. In other (integer) dimensions we expect no dynamo for any value of ξ.

4.1.5 Asymptotics for ξ Near ξ^* and 2

We now proceed to give estimates of the growth rate of the dynamo in the cases when ξ is near the critical value ξ^* above which dynamo is present, and when ξ is near its maximum possible value 2. What we need is an estimate of the largest solution w of (4.4), from which the corresponding growth rate z is immediately deduced through (3.9). We have argued in Sect. 4.1.3 that, as an order of magnitude estimate for the solution, we may take the largest zero w_0 of $K_\lambda(w)$, at least in some regions around $\xi = \xi^*$ and $\xi = 2$ respectively. Here we are going to derive the asymptotic behavior of w_0 for ξ near ξ^* and 2, and see that it predicts correctly the behaviour of the exact dynamo growth rate obtained numerically in [23].

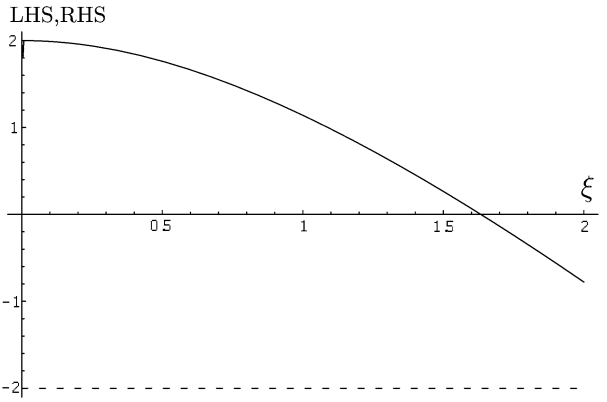

Fig. 9 Plot of $\tilde{\Lambda}_L(0)$ vs. $-\lambda$, multiplied by $2-\xi$, as functions of ξ. *Solid line* represents the left hand side ($\tilde{\Lambda}_L(0)$) and the *dashed line* is the right hand side which at two dimensions is -2

ξ Near ξ^* The case $\xi \searrow \xi^*$, corresponding to $\lambda \to 0$ along the imaginary axis, is somewhat simpler, it can be dealt with starting from the integral representation (4.8). Since $\xi > \xi^*$, the parameter λ is imaginary and we write $\lambda = i\tilde{\lambda}$ with $\tilde{\lambda} \in \mathbb{R}$, hence $K_{i\tilde{\lambda}}(w) = \int_0^\infty dt \exp(-w\cosh(t))\cos(\tilde{\lambda}t)$. Now $\cos(\tilde{\lambda}t)$ is positive near $t=0$ and it becomes negative for the first time only for $t > \pi/(2\tilde{\lambda})$. On the other hand the term $\exp(-w\cosh(t))$ is basically a double exponential and decays very fast for $w\cosh(t) > 1$. So in order to get for the previous integral a non-positive result, we need $w_0\cosh(\pi/(2\tilde{\lambda})) \sim 1$ implying $w_0 \sim \exp(-\pi/(2\tilde{\lambda}))$. Through (3.9) one deduces the behaviour $\ln z \sim c/\tilde{\lambda}$, and since $\tilde{\lambda} \propto (\xi - \xi^*)^{1/2}$ near ξ^* (the term under the square root in (3.10) is expected to have a simple root at $\xi = \xi^*$), we finally have

$$\ln z \propto (\xi - \xi^*)^{-1/2} \tag{4.12}$$

near ξ^*.

ξ Near 2 We now pass to the asymptotics of the case $\xi \to 2$. Under this limit λ diverges as $(2-\xi)^{-1}$, along the imaginary axis. The largest zero w_0 of $K_\lambda(w)$ is known [2, 6] to behave asymptotically for large purely imaginary λ as $w_0 = |\lambda|(1 + 2^{-1/3}A_1|\lambda|^{-2/3} + O(|\lambda|^{-4/3}))$ where $A_1 \approx -2.34$ is the first (smallest absolute value) negative zero of the Airy function Ai. Combining this with (3.9) and (3.10) we get

$$z \approx z_2 - c(2-\xi)^{2/3}, \quad c = |A_1|(d-1)^{1/3}z_2^{2/3} \tag{4.13}$$

valid for ξ near 2, where $c > 0$ is some constant of order unity and z_2 was introduced in (3.15).

4.2 Prandtl Number $P \to \infty$

For large Prandtl number the analysis proceeds exactly as in the previous section, except that we have a different Λ_L. From (8.30) and (8.27) we have, using the definition of ζ from (3.14),

$$\Lambda_L = \zeta - \frac{2}{d-1} - \frac{d}{2}. \tag{4.14}$$

There is now a branch cut originating from z_2 (defined in (3.15)) extending to infinity along the negative real axis. When $3 \leq d \leq 8$, z_2 is positive and the branch cut extends up to the positive value z_2 along the positive real axis, i.e. the spectrum has a continuous positive part for *all* $\xi \in [0, 2]$. Another major difference when comparing to the small Prandtl number case is that the spectrum is continuous also in the positive part.

We conclude that the dynamo is present for all ξ for large Prandtl numbers.

5 Some Remarks

5.1 Connection to the Schrödinger Operator Formalism

Here we would like to make a few comments regarding the large Prandtl number case, addressed principally to the reader familiar with the paper by Vincenzi [23] and the Schrödinger operator formalism used therein. For the definitions of ψ, U and m we refer the reader to that paper.

We note that same kind of piecewise analysis we have accomplished in the present work would have been possible also if we had first passed to the Schrödinger equation formalism. In that setup the existence of the dynamo would depend on whether the eigenvalues of the Schrödinger operator are negative or not. It may be explained heuristically why for a sufficiently large Prandtl number there is always a negative energy bounded state. Consider the zero energy Schrödinger equation

$$\psi''(r) = V(r)\psi(r), \tag{5.1}$$

where $V(r) = m(r)U(r)$ is the effective potential. The potential V behaves as $2/r^2$ at very short and long scales, but as $-4/r^2$ at the medium range, where the ranges correspond to the ones in this paper. The medium range solutions are $\sin(\sqrt{15}/2\log(r))$ and $\cos(\sqrt{15}/2\log(r))$. When the Prandtl number is increased, the medium range region is stretched, and it is clear that for sufficiently large Prandtl numbers the solutions cross zero an increasing number of times (see Fig. 10). According to a well known theorem, such a solution cannot be a ground state (see e.g. [20], pp. 90). In fact, the number of zeros of the solution (with nonzero derivative and excluding the zero at $r = 0$) is the number of negative energy states, which implies the existence of unbounded growth.

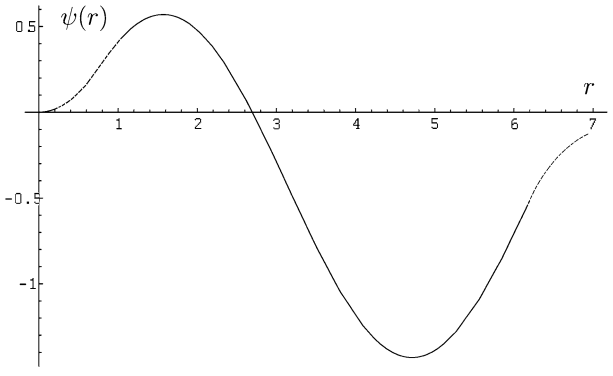

Fig. 10 Sketchy plot of the medium range zero energy solution $\sin(\sqrt{15}/2\log(r))$ crossing zero, implying the existence of a negative energy state. The *dashed lines* correspond to regions outside the medium range. As the range grows when increasing the Prandtl number, more zeros will emerge

5.2 Finite Magnetic Reynolds Number Effects

Let us finally touch upon some questions not discussed in the text. Our method allows us in principle, without further complications, to estimate the critical magnetic Reynolds number (dependent on velocity roughness exponent ξ and space dimension d) at which dynamo effect sets in, and the growth of the dynamo exponent with Reynolds number. However we get only a logarithmic estimate whose uncertainty is at least an order of magnitude or even two, which makes it not too useful. Notwithstanding, we would like to mention that the estimates we would obtain this way are hardly compatible with numerical results of [23], our thresholds being significantly lower. This issue is currently clarified with D. Vincenzi.

5.3 Exceptional Solutions

An other issue is that of the existence of "exceptional" dynamos. It seems to us that the "typical" dynamo (note that we consider here only the infinite magnetic Reynolds number case) corresponds to the situation when our $\xi > \xi^*$, in which case there is an infinite discrete spectrum of growing modes. However our equations do not exclude *a priori* the possibility of a single growing mode at some $\xi < \xi^*$. In fact, if we take for example, at a formal level, $d = 2.125$ then $\xi^* \approx 1.82$ and for $\xi' \leq \xi < \xi^*$ (where ξ' is some value of which we only need to know here that $\xi' < 1.77$), (4.4) will have, in what we have called the small z approximation (cf. (3.18)), a single solution $w_0 > 0$. If we take $\xi = 1.77$ then $w_0 \approx 0.077$ and $z \approx 8.8 \cdot 10^{-5} \ll 1$ in a self-consistent manner. However it remains to be known if such a solution is not just an artefact of our resolution method, and if not, then to see if one can construct a model where such solutions occur for the more physical value of $d = 3$.

A partial answer to these concerns is given in Appendix 4, where it is shown that for the system (2.7), (2.8), without the approximation (2.15), the absence of dynamo is quite straightforward, independently of the value of d, and doesn't require the finer analysis of Sect. 4.1.4.

6 Conclusions

The mean-field dynamo problem was considered in arbitrary space dimensions. We have shown that, to obtain the spectrum of the dynamo problem, (4.4) has to be solved for w, from which the growth rate z can be expressed through (3.9). The quantity Λ_L appearing in (4.4) is given, for small magnetic Prandtl numbers, by either (4.5) or (4.6), depending on which of the self-consistent conditions (3.17) or (3.18) is verified (note that this leaves a gap between, with no explicit formula). For large magnetic Prandtl number we have to use (4.14) instead.

It was observed that, in our model, the dynamo can only exist when $3 \leq d \leq 8$. The results for small Prandtl numbers were shown to confirm previous results [15, 23] obtained in three dimensions. For $d > 3$ a critical value for ξ was found, above which the dynamo is present, which is larger than the three dimensional critical value $\xi^* = 1$. Furthermore, in the vanishing Prandlt number limit we have obtained the asymptotic estimates (4.12) and (4.13), which are in good qualitative agreement with numerical simulations of [23].

For large Prandtl numbers it was shown that the dynamo exists for *all* ξ and that the spectrum is continuous. We hope our work will contribute to clarifying this somewhat controversial issue. The physical idea behind our explanations is that at large magnetic Prandtl number the magnetic field can feel the smooth scales of the fluid flow (they are not "wiped

out" by magnetic diffusivity), and correlations in the velocity field above the viscous scale l_ν won't do more harm to the dynamo than if we had a Batchelor type flow with no correlations of velocity at scales significantly larger than l_ν.

Our methods were based on approximating piecewise the evolution operator of the two-point function of the magnetic field. This approximation introduces inaccuracies and one may ask how these influence the fine details of our reasoning, which relied on non-trivial estimates. We think that the general picture sketched up should be valid for the exact problem also, based on the good agreement with available numerical data from the literature. Since for $\xi = \xi^*$ and $\xi = 2$ one can find the fastest growing mode explicitly, it should also be possible to do a perturbation theory around these points for the exact evolution operator, this is however left for future work.

Acknowledgements H.A. would like to thank P. Muratore-Ginanneschi and A. Kupiainen for useful comments, suggestions and discussions related to the problem at hand. P.H. would like to thank A. Kupiainen for inviting him to work at the Mathematics Department of Helsinki University, where most of this work has been done. The work of H.A. was partly supported by the Vilho, Yrjö and Kalle Väisälä foundation. We would also like to thank Dario Vincenzi for discussing his results with us and providing data from his simulations.

Appendix 1: PDE for the 2-Point Function of $\boldsymbol{B}$

We rewrite (1.5) as an Itô type SPDE (following the formalism of [17], Sect. 5)

$$dB_i + d\boldsymbol{w}\cdot\nabla B_i - \boldsymbol{B}\cdot\nabla dw_i - \kappa'\Delta B_i dt = 0, \tag{7.1}$$

where $\kappa' = \kappa + D/2$ with D defined as

$$D_{ij}(0) = D\delta_{ij}. \tag{7.2}$$

The new diffusion term in κ' emerges by advecting the magnetic field along the particle trajectories similarly as in the passive scalar case by using the Itô formula. It will cancel out eventually, as it should. We can express the above equation more conveniently by defining

$$db_i(t,\boldsymbol{x}) = -\mathcal{D}^x_{ijk}(B_j(t,\boldsymbol{x})dw_k(t,\boldsymbol{x})), \tag{7.3}$$

where $\mathcal{D}^x_{ijk} = \delta_{ij}\partial^x_k - \delta_{ik}\partial^x_j$.[2] The equation is then simply

$$dB_i - \kappa'\Delta B_i dt = db_i. \tag{7.4}$$

For a function F of fields $\boldsymbol{B}$, we have the (generalized) Itô formula,

$$\begin{aligned} dF(\boldsymbol{B}(t,\cdot)) = &\int d^d\boldsymbol{x}\frac{\delta F}{\delta B_i(\boldsymbol{x})}[\kappa'\Delta B_i dt + db_i] \\ &+ \frac{1}{2}\int d^d\boldsymbol{x}d^d\boldsymbol{y}\frac{\delta^2 F}{\delta B_i(\boldsymbol{x})\delta B_j(\boldsymbol{y})}\boldsymbol{E}(db_i(t,\boldsymbol{x})db_j(t,\boldsymbol{y})). \end{aligned} \tag{7.5}$$

The advecting velocity field is a time derivative of a Brownian motion on some state space, that is

$$\mathbb{E}dw_i(t,\boldsymbol{x})dw_j(t,\boldsymbol{y}) = dt\,D_{ij}(\boldsymbol{x}-\boldsymbol{y}), \tag{7.6}$$

[2] This is just a rewriting of the expression $\nabla\times(\boldsymbol{B}\times\boldsymbol{v})$ for incompressible fields $\boldsymbol{B}$ and $\boldsymbol{v}$.

where D_{ij} was defined in (1.8). This means that

$$\mathbb{E}db_i(t,\boldsymbol{x})db_j(t,\boldsymbol{y}) = \mathcal{D}^x_{ikl}\mathcal{D}^y_{jmn}\left(B_k(t,\boldsymbol{x})B_m(t,\boldsymbol{y})D_{ln}(\boldsymbol{x}-\boldsymbol{y})\right)dt. \tag{7.7}$$

We apply this to $F = u_i(t,\boldsymbol{x})u_j(t,\boldsymbol{y})$, denote $G_{ij}(\boldsymbol{x}-\boldsymbol{y}) = \mathbb{E}u_i(t,\boldsymbol{x})u_j(t,\boldsymbol{y})$ and use the decomposition $D_{ij}(\boldsymbol{x}-\boldsymbol{y}) = D\delta_{ij} - d_{ij}(\boldsymbol{x}-\boldsymbol{y})$ introduced in (1.10). Noting that terms proportional to dw disappear, we obtain the equation for the two point function:

$$\partial_t G_{ij} = 2\kappa\,\Delta G_{ij} + \mathcal{F}_{ij}, \tag{7.8}$$

and

$$\mathcal{F}_{ij} = d_{\alpha\beta}G_{ij,\alpha\beta} - d_{\alpha j,\beta}G_{i\beta,\alpha} - d_{i\beta,\alpha}G_{\alpha j,\beta} + d_{ij,\alpha\beta}G_{\alpha\beta}, \tag{7.9}$$

where the indices after commas denote partial derivatives with respect to $\boldsymbol{r} = \boldsymbol{x}-\boldsymbol{y}$. Note that this depends only on κ, not κ', i.e. the constant part $D\delta_{ij}$ of the structure function is absent. Using the decomposition (1.16) and the explicit form of the long distance velocity structure function (1.12) we get from (7.8) two equations for G_1 and G_2,

$$\partial_t G_1 = \frac{2\kappa}{r^2}(2G_2 + (d-1)r\partial_r G_1 + r^2\partial_r^2 G_1) + \mathcal{A}, \tag{7.10}$$

and

$$\partial_t G_2 = \frac{2\kappa}{r^2}(-2dG_2 + (d-1)r\partial_r G_2 + r^2\partial_r^2 G_2) + \mathcal{B}. \tag{7.11}$$

The symbols $\mathcal{A}$ and $\mathcal{B}$ are the terms arising from the interaction with the (long distance) velocity fields. Using the relations (1.18) for G_1 and G_2 in terms of H, their explicit form is as follows:

$$\begin{aligned}\frac{\mathcal{A}}{D_1 r^{-2+\xi}} &= \xi(d-1)(d-3+\xi)H \\ &\quad + (2-d-2d^2+d^3+(-5+d+2d^2)\xi+(1+d)\xi^2)r\partial_r H \\ &\quad + (2d(d-1)+(d+1)\xi))r^2\partial_r^2 H + (d-1)r^3\partial_r^3 H,\end{aligned} \tag{7.12}$$

$$\begin{aligned}-\frac{\mathcal{B}}{D_1 r^{-2+\xi}} &= -\xi(d-1)(2-\xi)H + ((1-d^2)+(d-5+2d^2)\xi+4\xi^2-\xi^3)r\partial_r H \\ &\quad + (d+1)(d-1+\xi)r^2\partial_r^2 H + (d-1)r^3\partial_r^3 H.\end{aligned} \tag{7.13}$$

Now we can just add the equations (7.10) and (7.11), and by using $G_1 + G_2 = (d-1)H$ we get

$$\begin{aligned}\partial_t H &= \xi(d-1)(d+\xi)D_1 r^{-2+\xi}H + (2(d+1)\kappa + (d^2-1+2\xi)D_1 r^{\xi})r^{-1}\partial_r H \\ &\quad + (2\kappa + (d-1)D_1 r^{\xi})\partial_r^2 H.\end{aligned} \tag{7.14}$$

Appendix 2: Computation of the Fraction C_L^-/C_L^+

By evaluating the matrix multiplications on the right hand side of (3.27), we can write the fraction C_L^-/C_L^+ as

$$\frac{C_L^-}{C_L^+} = -\frac{\partial h_L^+(1) - \Lambda_L h_L^+(1)}{\partial h_L^-(1) - \Lambda_L h_L^-(1)}, \tag{8.1}$$

where (again) for the sake of conciseness we write $\partial h(1) = \partial_\rho h(\rho)|_{\rho=1}$, and Λ_L can be written as the following nested expression:

$$\begin{cases} \Lambda_L = \dfrac{\partial h_M^+(1) + \Lambda_M \partial h_M^-(1)}{h_M^+(1) + \Lambda_M h_M^-(1)}, \\ \Lambda_M = -\dfrac{\partial h_M^+(a_i) - \Lambda_S h_M^+(a_i)}{\partial h_M^-(a_i) - \Lambda_S h_M^-(a_i)}, \\ \Lambda_S = \dfrac{\partial h_S(a_i)}{h_S(a_i)}. \end{cases} \tag{8.2}$$

This follows from defining

$$\begin{pmatrix} h_S \\ \partial h_S \end{pmatrix}_{a_i} = h_S(a_i) \begin{pmatrix} 1 \\ \Lambda_S \end{pmatrix} \tag{8.3}$$

and writing (3.27) as

$$\begin{pmatrix} C_L^+ \\ C_L^- \end{pmatrix} = c \begin{pmatrix} \partial h_L^- & -h_L^- \\ -\partial h_L^+ & h_L^+ \end{pmatrix}_1 \begin{pmatrix} h_M^+ & h_M^- \\ \partial h_M^+ & \partial h_M^- \end{pmatrix}_1 \begin{pmatrix} \partial h_M^- & -h_M^- \\ -\partial h_M^+ & h_M^+ \end{pmatrix}_{a_i} \begin{pmatrix} 1 \\ \Lambda_S \end{pmatrix}, \tag{8.4}$$

where $h_S(a_i)$ is absorbed in the coefficient. We have defined above a constant c which gets cancelled in the end of computations. It will be used below as well as a generic constant that does not affect the final results. Multiplying the last matrix with the vector, we define similarly

$$\begin{pmatrix} \partial h_M^- & -h_M^- \\ -\partial h_M^+ & h_M^+ \end{pmatrix}_{a_i} \begin{pmatrix} 1 \\ \Lambda_S \end{pmatrix} = \begin{pmatrix} \partial h_M^- - \Lambda_S h_M^- \\ -\partial h_M^+ + \Lambda_S h_M^+ \end{pmatrix}_{a_i} = c \begin{pmatrix} 1 \\ \Lambda_M \end{pmatrix}, \tag{8.5}$$

that is,

$$\Lambda_M = -\frac{\partial h_M^+(a_i) - \Lambda_S h_M^+(a_i)}{\partial h_M^-(a_i) - \Lambda_S h_M^-(a_i)}. \tag{8.6}$$

Doing this again for the second matrix, we obtain similarly

$$\Lambda_L = \frac{\partial h_M^+(1) + \Lambda_M \partial h_M^-(1)}{h_M^+(1) + \Lambda_M h_M^-(1)} \tag{8.7}$$

and finally

$$\frac{C_L^-}{C_L^+} = -\frac{\partial h_L^+(1) - \Lambda_L h_L^+(1)}{\partial h_L^-(1) - \Lambda_L h_L^-(1)}. \tag{8.8}$$

We are interested in the leading order behavior of the fraction C_L^-/C_L^+ only, so we need to determine what happens to Λ_M as P approaches zero or infinity. It turns out that either $\Lambda_M \to 0$ or $\Lambda_M \to \pm\infty$, so to the leading order,

$$\Lambda_L = \frac{\partial h_M^{\pm}(1)}{h_M^{\pm}(1)} \,. \tag{8.9}$$

2.1 $P \ll 1$

Below the suspension dots denote higher order terms in powers of P (or P^{-1} for large Prandtl numbers). Recall from (3.22) and (2.13) that

$$a_1 = l_v/l_\kappa = \left(\frac{d-1}{2}P\right)^{1/\xi} . \tag{8.10}$$

The short range solution was

$$h_S(\rho) = \rho^{-d/2}\, I_{d/2}\,(\alpha\rho)\,, \tag{8.11}$$

with a temporary notation $\alpha = \sqrt{(z + 2P^{1-2/\xi}(2-d-d^2))/(d-1)}$ and note that $|\alpha|$ behaves as $P^{1/2-1/\xi}$. Using standard relations of Bessel functions [13] and using the definition for Λ_S in (8.2), we have

$$\Lambda_S = \frac{\partial h_S(a_1)}{h_S(a_1)} = \alpha \frac{I_{1+d/2}\big((\frac{d-1}{2}P)^{1/\xi}\alpha\big)}{I_{d/2}\big((\frac{d-1}{2}P)^{1/\xi}\alpha\big)}. \tag{8.12}$$

Since P is small and the arguments of the Bessel functions above scale as $P^{1/2}$, we can use the expansion

$$I_{d/2}(u) = u^{d/2}\left(\frac{2^{-d/2}}{\Gamma(1+d/2)} + \frac{2^{-2-d/2}}{\Gamma(2+d/2)}u^2 + \mathcal{O}(u^4)\right) \tag{8.13}$$

(and a corresponding one when the order parameter is $1 + d/2$) to conclude that

$$\Lambda_S = cP^{1-1/\xi} + \cdots . \tag{8.14}$$

At this point our analysis splits according to which approximation (3.19) or (3.20) we use for $h_{M,1}^{\pm}$, i.e. we treat separately the cases of small and large z. Finally when $\xi = 2$ the problem can be treated for any z.

2.1.1 Large z Case

The medium range solutions in the large z case, (3.19), are

$$h_{M,1}^{\pm}(\rho) = \rho^{-d/2}\begin{cases} I_{d/2} \\ K_{d/2} \end{cases}\left(\sqrt{\beta}\rho\right), \tag{8.15}$$

with $\beta = z/(d-1)$. The leading order behavior is

$$\begin{cases} h_M^+(a_1) = c + \cdots, \\ \partial h_M^+(a_1) = cP^{1/\xi} + \cdots, \\ h_M^-(a_1) = cP^{-d/\xi} + \cdots, \\ \partial h_M^-(a_1) = cP^{-1/\xi - d/\xi} + \cdots . \end{cases} \tag{8.16}$$

Using these on Λ_M as given by (8.6), we see that to leading order

$$\Lambda_M = cP^{d/\xi+1}, \tag{8.17}$$

which goes to zero. Therefore we have

$$\Lambda_L \sim \frac{\partial h_M^+(1)}{h_M^+(1)} = \sqrt{\frac{z}{d-1}}\frac{I_{1+d/2}\left(\sqrt{\frac{z}{d-1}}\right)}{I_{d/2}\left(\sqrt{\frac{z}{d-1}}\right)}. \tag{8.18}$$

Note that, notwithstanding the fractional powers appearing above, Λ_L is a single valued function, indeed near $z=0$ it behaves as $\Lambda_L \approx z/(d-1)$. One also notes that in the large z case Λ_L is always positive, since the Bessel functions I are positive for positive parameter and argument.

2.1.2 Small z Case

We may perform a similar analysis for the small z approximation, based on (3.20),

$$h_{M,1}^{\pm}(\rho) = \rho^{-d/2}\begin{cases} J_{d/\xi} \\ Y_{d/\xi} \end{cases}\left(\gamma\rho^{\xi/2}\right), \tag{8.19}$$

with $\gamma = 2\sqrt{d/\xi+1}$. The leading order behavior is

$$\begin{cases} h_M^+(a_1) = c + \cdots, \\ \partial h_M^+(a_1) = cP^{1-1/\xi} + \cdots, \\ h_M^-(a_1) = cP^{-d/\xi} + \cdots, \\ \partial h_M^-(a_1) = cP^{-1/\xi-d/\xi} + \cdots. \end{cases} \tag{8.20}$$

Using these on Λ_M (cf. (8.6)), we see that once again Λ_M behaves at leading order as given in (8.17), meaning that it goes to zero as P goes to zero. Therefore we have

$$\Lambda_L \sim \frac{\partial h_M^+(1)}{h_M^+(1)} = -\xi\sqrt{d/\xi+1}\frac{J_{d/\xi+1}(2\sqrt{d/\xi+1})}{J_{d/\xi}(2\sqrt{d/\xi+1})}. \tag{8.21}$$

2.1.3 Case of $\xi = 2$

In the particular case of $\xi = 2$ the medium range solution can be explicitly calculated for any z, and we have

$$h_{M,1}^{\pm}(\rho) = \rho^{-d/2}\begin{cases} J_{d/2} \\ Y_{d/2} \end{cases}\left(\sqrt{\beta}\rho\right), \tag{8.22}$$

where now $\beta = 2(d+2) - z/(d-1)$. The approximations in (8.16) or (8.20) (for $\xi = 2$ those two coincide) are valid uniformly as ξ goes to 2, so when β is of order unity, the leading order behaviour (8.17) is valid. Note that for $z = z_2$ we indeed have β of order unity. Now one deduces that $\Lambda_L = -\sqrt{\beta}J_{d/2+1}(\sqrt{\beta})/J_{d/2}(\sqrt{\beta})$, and for $z = z_2$ one finds $\sqrt{\beta} = (d^2-d+4)/4/(d-1)$. One can then verify numerically that for $\xi = 2$ and $z = z_2$ and relevant values of d (between 3 and 8 inclusive) we have $\tilde{\Lambda}_L > 0$. By continuity, positivity carries over to values of ξ close to 2 and the corresponding dynamo growth rate z. This permits us to use near $\xi = 2$ the upper bound w_0' on the largest solution of (4.4), and obtain the asymptotic behaviour of Sect. 4.1.5.

2.2 $P \gg 1$

Now we have $a_2 = ((d-1)P/2)^{-1/2}$. The short range solution is in this case

$$h_S(\rho) = \rho^{-d/2}\, I_{d/2}(\sqrt{P}\alpha'\rho), \tag{8.23}$$

with

$$\alpha' = \frac{1}{\sqrt{2}}\sqrt{z + 2(2 - d - d^2)}. \tag{8.24}$$

Similarly to the $P \ll 1$ case,

$$\Lambda_S = \sqrt{P}\alpha' \frac{I_{1+d/2}(\sqrt{\frac{2}{d-1}}\alpha')}{I_{d/2}(\sqrt{\frac{2}{d-1}}\alpha')} = c\sqrt{P} + \cdots. \tag{8.25}$$

The medium range solutions are now power laws,

$$h_M^{\pm} = \rho^{-d/2-2/(d-1)\pm\delta}, \tag{8.26}$$

where

$$\delta = \frac{\sqrt{d(d^3 - 10d^2 + 9d + 16) + 4(d-1)z}}{2(d-1)}. \tag{8.27}$$

Since $\partial h_M^{\pm}(a_2) \propto \sqrt{P} h_M^{\pm}(a_2)$,

$$\partial h_M^{\pm}(a_2) - \Lambda_S h_M^{\pm}(a_2) = c\sqrt{P} h_M^{\pm}(a_2) + \cdots, \tag{8.28}$$

that is,

$$\Lambda_M = c\frac{h_M^{+}(a_2)}{h_M^{-}(a_2)} + \cdots = c\frac{1}{P} + \cdots. \tag{8.29}$$

This goes to zero as $P \to \infty$, and we have

$$\Lambda_L \to \frac{\partial h_M^{+}(1)}{h_M^{+}(1)} = \zeta - \frac{2}{d-1} - \frac{d}{2}, \tag{8.30}$$

where ζ was defined in (3.14). In fact we wouldn't have needed to worry if the limit of Λ_M was infinite or zero. The difference would only be a different sign of ζ, which doesn't affect anything since it is the presence of the branch cut alone which determines the positive part of the spectrum.

Appendix 3: Some Sturm-Liouville Theory

Consider the following general second order linear eigenvalue problem, where a, b, c are positive functions and $z \in \mathbb{R}$:

$$a(\rho)h''(\rho) + b(\rho)h'(\rho) + c(\rho)h(\rho) = zh(\rho). \tag{9.1}$$

Introduce $g = h'/h$, then g verifies the first order non-linear (Riccati) differential equation

$$g' = \frac{z - c - bg - ag^2}{a}. \tag{9.2}$$

Note that a zero of h corresponds to a pole of g, and the pole is always such that as ρ increases g goes to $-\infty$ and comes back at $+\infty$ (since if h is positive before crossing zero then its derivative must be negative and vice versa).

3.1 Monotonicity of Solutions in z

Consider for (9.1) the initial condition $h'(0) = 0$ and $h(0) > 0$ which in particular implies $g(0) = 0$. Now consider (9.1) and (9.2) for two different values of z, say z_1 and z_2, and denote the corresponding solutions by h_1, g_1 and h_2, g_2 respectively. We show that if $z_1 > z_2$, then $g_1(\rho) > g_2(\rho)$ for ρ less than the first zero of h_2.

This can be seen as follows. First, the assertion is true near $\rho = 0$ since $g_1'(0) = (z_1 - c(0))/a(0) > (z_2 - c(0))/a(0) = g_2'(0)$ while $g_1(0) = g_2(0) = 0$. Now suppose that at some point the ordering of g_1 and g_2 changes, this means that the two have to cross, i.e. for some ρ we have $g_1(\rho) = g_2(\rho) = G$. However at this point $g_1'(\rho) = (z_1 - c(\rho) - b(\rho)G - a(\rho)G^2)/a(\rho) > (z_2 - c(\rho) - b(\rho)G - a(\rho)G^2)/a(\rho) = g_2'(\rho)$, meaning that g_1 cannot cross g_2 downwards, which is a contradiction.

Below we give a few specific applications of these results to our problem. Some of these are used in the main text.

3.1.1 Position of First Zero of h Increases with z

From the above it also follows that the first zero of h_1 is larger than the first zero of h_2. Indeed h_2 has, obviously, no zero before its first zero. Thus g_2 doesn't go to $-\infty$ before that point, implying that g_1 neither since $g_1 > g_2$. But then h_1 has no zero either before the first zero of h_2.

A particularly useful application of this is to use the position of the first zero of the solution with $z = 0$ as a lower bound on the first zero of any solution for $z > 0$.

3.1.2 At small Prandtl, Λ_L is Non-Singular and Increases with z

We may apply the above to the case when (9.1) corresponds to the small Prandtl approximation (2.15b) of $\mathcal{M}_M$. For $P \to 0$ the lower (i.e. left) boundary condition for h_M becomes $h_M'(0) = 0$. The case $z = 0$ can be explicitly solved and we get $h_M^0(\rho) := h_M^{z=0}(\rho) = \rho^{-d/2} J_{d/\xi}(2\sqrt{d/\xi + 1}\rho^{\xi/2})$. What needs to be seen is that h_M^0 does not have zeros between 0 and 1, equivalent to $J_{d/\xi}$ not having zeros between 0 and $2\sqrt{d/\xi + 1}$. The latter follows from the fact that $j_{\nu,1} > 2\sqrt{\nu + 1}$ for $\nu \geq 0$ (where $j_{\nu,1}$ is the first positive zero of the Bessel function of index ν), which may be seen from the plot in Fig. 11, in conjunction with the fact that we have $j_{\nu,1} > \nu$ [24].

In view of Appendix 3.1.1 this allows us to conclude that $h_M(\rho)$ doesn't have zeros for any $z \geq 0$ for $\rho \in [0, 1]$, so $\Lambda_L = h_M'(1)/h_M(1)$ is finite and grows with z for $z \geq 0$.

Finally let us point out that h_M^0 *does* have zeros (for $\rho > 1$ though), and this is due to the presence of the term $\xi(d-1)(d+\xi)\rho^{\xi-2}h_M$ in (2.15b). Without this term we would have $h_M^0 = 1$, and obviously it wouldn't have zeros. However the term in question corresponds to the effect of the velocity field *below* the magnetic diffusive scale l_κ. Thus it is quite surprising that such a contribution makes it completely *non* self evident—or even seemingly fortuitous—that Λ_L is indeed always monotonously increasing and finite.

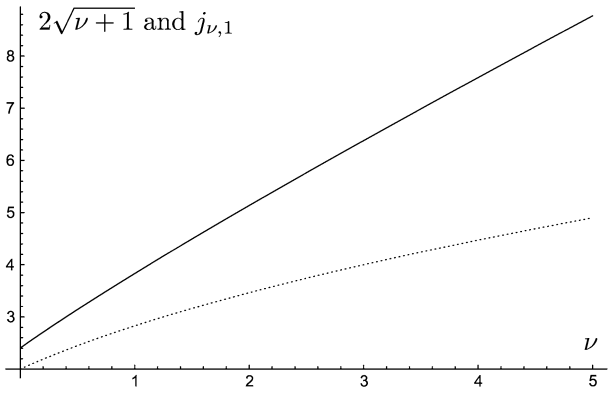

Fig. 11 Plot of $j_{\nu,1}$ (*solid line*) and $2\sqrt{\nu+1}$ (*dashed line*) for $\nu = 0 \ldots 5$. For $\nu > 5$ we have $j_{\nu,1} > \nu > 2\sqrt{\nu+1}$ by [24]

3.1.3 Nodeless Zero Mode Implies no $z > 0$ Eigenfunction

Along the same lines one can prove for our case the standard lore of Sturm-Liouville theory that if the zero mode ($z = 0$ solution) has no zeros, then there is no eigenfunction with $z > 0$.

The idea is that while the zero mode decays near infinity as a power law, any eigenfunction h_1 for $z > 0$ has to decay exponentially, so it will be below the zero mode. On the other hand, from (9.1) one deduces that $h''(0)$ grows with z, so that h_1 has to be larger than the zero mode near $\rho = 0$. This would imply that the two have to cross in the sense that h_2 comes from above and goes below the zero mode, but at the crossing point g_1 would be less than that of the zero mode, which contradicts the above said.

3.2 Consequences for Modified Bessel Function

We wish to prove here that, for pure imaginary λ, the slope of $\rho K'_\lambda(\rho)/K_\lambda(\rho)$ is bounded from above by -1 for all $\rho > 0$.

Using notation from the previous subsections, introduce $f(\rho) = \rho g(\rho)$. Then (9.2) translates to $f' = [(z-c)\rho + (a/\rho - b)f - (a/\rho)f^2]/a$. Applied to the particular case of the modified Bessel equation with parameter λ

$$\rho^2 h'' + \rho h' - \rho^2 h = \lambda^2 h,$$

i.e. when $a(\rho) = \rho^2$, $b(\rho) = \rho$, $c(\rho) = -\rho^2$ and $z = \lambda^2$, we obtain

$$f' = (\rho^2 + \lambda^2 - f^2)/\rho. \tag{9.3}$$

Solving (9.3) for $f' = -1$ gives $f^2 = s(\rho)^2$ where we define $s(\rho) = -[(\rho + 1/2)^2 + \lambda^2 - 1/4]^{1/2}$. Moreover when $f^2 > s^2$ then $f' < -1$.

We now take $f = \rho K'_\lambda(\rho)/K_\lambda(\rho)$ in the case when λ is pure imaginary. Then, for large ρ, asymptotically $f(\rho) - s(\rho) \sim -(1 - 4\lambda^2)/(16\rho^2) < 0$, the last inequality being guaranteed by the fact that we consider the case when λ is pure imaginary and hence $\lambda^2 \leq 0$. This means that for large ρ asymptotically $f < s$.

Using the fact that f is continuous, if f were to become larger than s for some finite ρ, necessarily it would pass through $f = s$, but at that point we would have $f' = -1 > s'$ (the inequality holding for λ pure imaginary), which is a contradiction to the fact that for larger ρ we should have $f < s$.

This proves that $f < s \leq 0$ when s is real, and thus $f^2 > s^2$ for all $\rho \geq 0$, whence $f' < -1$ for $\rho \geq 0$.

3.3 Real Spectrum

Though we do not consider $\mathcal{M}$ to be self-adjoint, its spectrum is always real, for the following reason.

Since $\mathcal{M}$ is a second order differential operator we may conjugate it by a multiplication operator (by a "function" which is known in the theory of diffusion processes as the speed measure) to get a symmetric operator $\tilde{\mathcal{M}}$, and taking into account the boundary conditions we have (we see that for any $z \in \mathbb{C} \setminus \mathbb{R}_-$ the solution of $\tilde{\mathcal{M}}h = zh$ which verifies the boundary conditions is a twice differentiable function with zero derivative at $\rho = 0$ and exponentially decaying as $\rho \to \infty$, so h is also in the domain of $\tilde{\mathcal{M}}^\dagger$), we can use the same trick as for self-adjoint operators: suppose $\tilde{\mathcal{M}}h = zh$ and write $\int \bar{h}\tilde{\mathcal{M}}h = z\int \bar{h}h$, now take the complex conjugate of both sides, and since $\tilde{\mathcal{M}}$ is real and symmetric, we have $\int \bar{h}\tilde{\mathcal{M}}h = \bar{z}\int \bar{h}h$, showing that $z = \bar{z}$, i.e. that z is real.

Appendix 4: Exact Results for $P = 0$

Here we want to study more rigorously the case of $P = 0$. In this case we can find exactly the zero mode of (2.7). For λ real (recall its definition from (3.10)) we show that the Appendix 3.1.3 we conclude that there is no dynamo effect in this case. On the other hand for λ pure imaginary the zero mode has an infinity of nodes.

Recalling (2.11), first we have to solve for the zero mode of the operator $[\xi(d-1)\times(d+\xi)\rho^{\xi-2} + (d^2-1+2\xi)\rho^{\xi-1}\partial_\rho + (d-1)\rho^\xi\partial_\rho^2] + [(d^2-1)\rho^{-1}\partial_\rho + (d-1)\partial_\rho^2]$. At zero Prandtl number the boundary condition is to have finite limit at $\rho = 0$. The appropriate solution is

$$(\rho^\xi + 1)^{(d-3)/(d-1)}\,{}_2F_1(a, b; c; -\rho^\xi),$$

where ${}_2F_1$ is the hypergeometric function and

$$\begin{cases} a = \dfrac{2(d-2)\xi + d(d-1) + (2-\xi)(d-1)\lambda}{2\xi(d-1)}, \\ b = \dfrac{2(d-2)\xi + d(d-1) - (2-\xi)(d-1)\lambda}{2\xi(d-1)}, \\ c = \dfrac{d+\xi}{\xi}. \end{cases} \tag{10.1}$$

Let us start with the case of λ real. Without loss of generality, we may suppose $\lambda > 0$ (or otherwise exchange a and b, since the hypergeometric function is symmetric in those arguments). Notice that $2(d-2)\xi + d(d-1) > 0$ and $[2(d-2)\xi + d(d-1)]^2 - [(2-\xi)(d-1)\lambda]^2 = 2d^2(d-1)^2 - 8\xi^2(d-2) \geq 2[d^2(d-1)^2 - 16(d-2)] > 0$, implying $b > 0$.

Notice also $2(d-1)(d+\xi) - [2(d-2)\xi + d(d-1)] = d(d-1) + 2\xi > 0$ implying $c - b > 0$.

Now write the following integral representation of the hypergeometric function:

$${}_2F_1(a, b; c; x) = \frac{\Gamma(c)}{\Gamma(b)\Gamma(c-b)}\int_0^1 \frac{t^{b-1}(1-t)^{c-b-1}}{(1-tx)^a}dt \quad (c > b > 0)$$

whence ${}_2F_1(a, b; c; x) > 0$ for any $x < 1$ and $c > b > 0$.

Since we have shown above $c > b > 0$ and since our $x < 0$, this proves that the zero mode has no zeros, and hence there cannot be a dynamo effect.

For λ pure imaginary it is possible to make a large ρ development using the so called linear transformation formula

$$
\begin{aligned}
{}_2F_1(a,b;c;-x) = {} & \frac{\Gamma(c)\Gamma(b-a)}{\Gamma(b)\Gamma(c-a)} x^{-a}\, {}_2F_1(a,1-c+a;1-b+a;-1/x) \\
& + \frac{\Gamma(c)\Gamma(a-b)}{\Gamma(a)\Gamma(c-b)} x^{-b}\, {}_2F_1(b,1-c+b;1-a+b;-1/x). \qquad (10.2)
\end{aligned}
$$

Since a and b are complex conjugates in the case of pure imaginary λ, the large x asymptotics can be written as ${}_2F_1(a,b;c;-x) \sim \Re(\frac{\Gamma(c)\Gamma(b-a)}{\Gamma(b)\Gamma(c-a)} x^{-a})$, which has an infinity of zeros since a has an imaginary part.

References

1. Adzhemyan, L.T., Antonov, N.V., Mazzino, A., Muratore-Ginanneschi, P., Runov, A.V.: Pressure and intermittency in passive vector turbulence. Europhys. Lett. **55**(6), 801 (2001). arXiv:nlin/0102017
2. Balogh, C.B.: Asymptotic expansions of the modified Bessel function of the third kind of imaginary order. SIAM J. Appl. Math. **15**(5), 1315 (1967)
3. Chaves, M., Eyink, G., Frisch, U., Vergassola, M.: Universal decay of scalar turbulence. Phys. Rev. Lett. **86**, 2305 (2001)
4. Chertkov, M., Falkovich, G., Kolokolov, I., Lebedev, V.: Statistics of a passive scalar advected by a large-scale two-dimensional velocity field: analytic solution. Phys. Rev. E **51**, 5609 (1995)
5. Chertkov, M., Falkovich, G., Kolokolov, I., Vergassola, M.: Small-scale turbulent dynamo. Phys. Rev. Lett. **83**, 4065 (1999)
6. Dunster, T.M.: Bessel functions of purely imaginary order with an application to second-order linear differential equations having a large parameter. SIAM J. Math. Anal. **21**(4), 995–1018 (1990)
7. Engel, K.-J., Nagel, R.: One-Parameter Semigroups for Linear Evolution Equations. Springer, Berlin (2000)
8. Falkovich, G., Gawedzki, K., Vergassola, M.: Particles and fields in fluid turbulence. Rev. Mod. Phys. **73**, 913–975 (2001)
9. Gawedzki, K., Kupiainen, A.: Universality in turbulence: An exactly soluble model. In: Grosse, H., Pittner, L. (eds.) Low-Dimensional Models in Statistical Physics and Quantum Field Theory, pp. 71–105. Springer, Berlin (1996). arXiv:chao-dyn/9504002
10. Gawedzki, K.: Easy turbulence. In: Saint-Aubin, Y., Vinet, L. (eds.) Theoretical Physics at the End of the Twentieth Century. Lecture Notes of the CRM Summer School, Banff, Alberta (CRM Series in Mathematical Physics). Springer, New York (2001). arXiv:chao-dyn/9907024
11. Gawedzki, K., Horvai, P.: Sticky behavior of fluid particles in the compressible Kraichnan model. J. Stat. Phys. **116**(5,6), 1247–1300(54) (2004)
12. Goldston, R.J., Rutherford, P.H.: Introduction to Plasma Physics. IOP Publishing, Bristol (1995)
13. Gradshteyn, I.S., Ryzhik, I.M.: Table of Integrals, Series and Products. Academic Press, New York (1965)
14. Hakulinen, V.: Passive advection and the degenerate elliptic operators M_n. Commun. Math. Phys. **235**(1), 1–45 (2003). arXiv:math-ph/0210001
15. Kazantsev, A.P.: Enhancement of a magnetic field by a conducting fluid flow. Sov. Phys. JETP **26**, 1031 (1968)
16. Kraichnan, R.H.: Small scale structure of a scalar field convected by turbulence. Phys. Fluids **11**, 945–953 (1968)
17. Kupiainen, A.: Statistical theories of turbulence. In: Lecture Notes from Random Media 2000. Madralin, June (2000). http://www.helsinki.fi/~ajkupiai/papers/poland.ps
18. Le Jan, Y., Raimond, O.: Integration of Brownian vector fields. Ann. Probab. **30**(2), 826–873 (2002). arXiv:math.PR/9909147
19. Lunardi, A.: Analytic Semigroups and Optimal Regularity in Parabolic Problems. Birkhäuser, Basel (1995)

20. Reed, M., Simon, B.: Methods of Modern Mathematical Physics IV: Analysis of Operators. Academic Press, London (1978)
21. Shraiman, B., Siggia, E.: Lagrangian path integrals and fluctuations in random flow. Phys. Rev. E **49**, 2912 (1994)
22. Vergassola, M.: Anomalous scaling for passively advected magnetic fields. Phys. Rev. E **53**, R3021–R3024 (1996)
23. Vincenzi, D.: The Kraichnan-Kazantsev dynamo. J. Stat. Phys. **106**, 1073–1091 (2002)
24. Watson, G.N.: In: Theory of Bessel Functions, p. 485. Cambridge University Press, Cambridge (1962)